

NON-PARAMETRIC BAYESIAN STATE SPACE ESTIMATOR

In both Chapters 3 and 4, we demonstrated that it is feasible to learn a POMDP policy from human teachers. Further, by adding a simple binary reward function we were able to take into consideration the quality of these demonstrations provided by the teachers. With this, we showed that our Reinforcement Learning extension, RL-PbD-POMDP was able to yield improved policies even when provided with a limited number of demonstrations taken from the worst teachers.

Both tasks from the previous two chapters (search for wooden block on a table and peg-in-hole) fall into the category of goal oriented **active-localisation**. In general, the localisation problem consists of estimating position parameters given noisy observations whereas active-localisation refers to a policy which actively takes actions to acquire information to decrease the uncertainty of the position estimate. In localisation, the model of the world also known as the **map** is considered **prior knowledge**. This assumption constrains localisation to an environment in which schematics exist and can be used as the world model such as in the case of offices and buildings. If the map is not known a priori, then Simultaneous Localisation And Mapping (**SLAM**) algorithms have to be used instead of localisation. Typically, the map consists of a set of features also known as landmarks which can be identified by sensors, and SLAM algorithms maintain a filtered joint probability distribution over both the agent's and features' position which is updated in accordance to a generic Bayesian State Space Filter (BSSF) (see Figure 2.5 on page 20).

In this Chapter, we consider an agent tasked with searching for a set of objects on a *Table* world (see Figure 5.1), in which exteroceptive feedback is extremely limited. The agent can only sense an object after making physical contact with it (bumping into it). The agent's uncertainty of its location and that of the object is encoded by probability distributions $P(\cdot)$, which at initialisation are known as the agent's prior beliefs.

Figure 5.1 illustrates a particular instance of the agent's beliefs. The agent is currently located in the bottom table and has only a limited knowledge of its location, somewhere near the right edge of the table.

As the agent explores the world, it integrates all sensing information at each time step and updates its prior beliefs to posteriors (the result of the prior belief

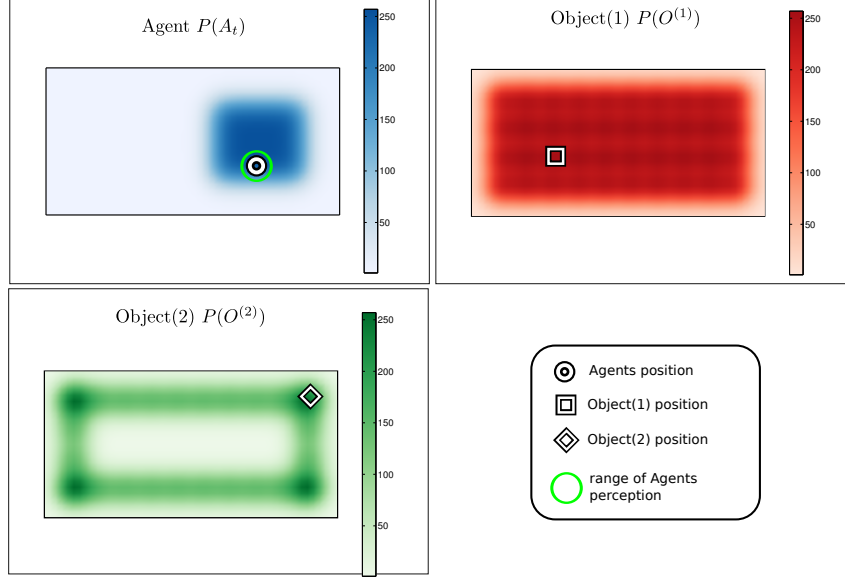


Figure 5.1: *Table Environment* Table World (delimited by the black rectangle), viewed from above, and the agent’s beliefs. There are three different probability density functions present on the table. The blue represents the believed location of the agent, the red and green probability distributions are associated with object 1 and 2. The white shapes in each figure represent the true location of each associated object or agent.

after integrating motion and sensory information). All current SLAM methods are limited in that they only consider uncertainty induced by sensing inaccuracy inherent in the sensor and motion models. In our setting as the sensory information is strictly haptic, we can confidently assume no measurement noise. In the search task illustrated in Figure 5.1, the beliefs and sparse measurement information available to the agent are the source of the uncertainty which is, the absence of positive object measurements. This is known as **negative information** (Sebastian Thrun and Fox, 2005, p.313) Thrun (2002); Hoffman et al. (2005). Thus SLAM methodologies which use the **Gaussian error** between the predicted and estimated position of features, such as in the case of EKF-SLAM and Graph-SLAM, will not work well in this setting.

The EKF SLAM algorithm, [...], can only process positive sightings of landmarks. It cannot process negative information that arises from the absence of landmarks. -Probabilistic Robotics (Sebastian Thrun and Fox, 2005, p.313)-

In addition to the negative sensing information, the original beliefs depicted in Figure 5.1 are **non-Gaussian** and **multi-modal**. We make **no assumption** regarding the form the beliefs can take. This implies that the joint distribution can no longer be parameterised by a Multivariate Gaussian. This is an assumption made in many SLAM algorithms, notably EKF-SLAM, and allows for a closed form solution to the state estimation problem. Without the Gaussian assumption no closed form solution to the filtering problem is feasible. Using stan-

Attributes & Assumptions

- Non-Gaussian joint distribution, no assumptions are made with respect to its form.
- Mostly negative information available (absence of positive sightings of the landmarks).
- Joint distribution volume grows exponentially with respect to the number of objects and states.
- Joint distribution volume is dense, there is a lot of uncertainty.

Figure 5.2: Assumptions and attributes which have to be fulfilled by our Bayesian State Space Filter.

standard non-parametric methods (Kernel Density, Gaussian Process, Histogram,...) to represent or estimate the joint distribution becomes unrealistic after a few dimensions or additional map features. FastSLAM could be a potential candidate, however as it parameterises the position uncertainty of the agent by a particle filter and each particle has its own copy of the map, the memory demand will become significant. For planning purposes we would also want to have a single representation of the marginals. Figure 5.2 summarises the desirable attributes and assumptions for our filter.

The main contribution of our work and the importance to the field of Artificial Intelligence

An accurate estimate of the agent’s belief space is a necessary precondition before planning or reasoning can be carried out. In a wide range of Artificial Intelligence (AI) applications the agent’s beliefs are discrete. This non-parametric representation is the most unconstraining but comes at a cost. The parameterisation of the belief’s joint distribution grows at the rate of a double exponential. We propose a Bayesian state estimator which delivers the same filtered beliefs as a traditional filter but without explicitly parametrising the joint distribution. Through the memorising of the measurement likelihood functions having been applied on the joint distribution and by taking advantage of their structure, we achieve a filter which grows linearly as opposed to exponentially in both time and space complexity. We refer to our novel filter as the Measurement Likelihood Memory Filter (MLMF) it keeps track of the history of measurement likelihood functions, referred to as the memory, which have been applied on the joint distribution. The MLMF filter allows to efficiently process negative information. To the authors knowledge there has been little research on the integration of negative information in a SLAM setting. Previous work considered the case of active localisation [Hoffmann et al. \(2006\)](#). The incorporation of negative information is useful in many contexts and in particular in Bayesian Theory of Mind [Bake et al. \(2011\)](#), where the reasoning process of a human

is inferred from a Bayesian Network and in our own work [de Chambrier and Billard \(2013\)](#) where we model the search behaviour of a intentionally blinded human. In such a setting much negative information is present and an efficient belief filter is required. Our MLMF is thus applicable to the SLAM & AI community in general and to the cognitive community which models human or agent behaviours through the usage of Bayesian state estimators.

By using this new representation we implement a set of passive search trajectories through the state space and demonstrate, for a discretised state space, that our novel filter is optimal with respect to the Bayesian criteria (the successive filtered posteriors are exact and not an approximation with respect to Bayes rule). We provide an analysis of the space and time complexity of our algorithm and prove that it is always more efficient even when considering worst case scenarios. Lastly we consider an Active-SLAM setting and evaluate the effect of how constraining the size of the number of memorised likelihood functions impacts the decision making process of a greedy one-step look-ahead planner.

5.1 Outline

The remaining part of this Chapter is structured as follows:

- [5.2 Background](#): Review of three prominent SLAM algorithms and their assumptions and an overview of active-localisation and exploration methods used with SLAM.
- [5.3 Bayesian State Space Estimation](#): Introduction to EKF-SLAM and why it is not suitable when mostly negative information is available. Description of the Histogram-SLAM algorithm and the assumptions which can be exploited.
- [5.4 Measurement Likelihood Memory Filter](#): Mathematical derivation of the MLMF, time and space complexity evaluation and extension to the scalable-MLMF.
- [5.5 Evaluation](#) We numerically evaluate the time complexity of the scalable-MLMF and check its assumptions. We investigate the filter's sensitivity with respect to its parameters in an Active-SLAM setting.
- [5.6 Conclusion](#)
- [5.7 Appendix](#)

5.2 Background

5.2.1 SLAM

Estimating the location or state parameters of a mobile agent whilst simultaneously building a map of the environment has been regarded as one of the most important problems to be solved for agents to achieve true autonomy. It is a necessary precondition for any agent to have an estimation of the world at its disposal which accurately encompasses all knowledge and related uncertainties. There has been much research surrounding the field of Simultaneous Localisation And Mapping (SLAM) which branches out into a wide variety of sub-fields dealing with problems from building accurate noise models of the agent sensors [Plagemann et al. \(2007\)](#), to determining which environmental feature caused a particular measurement, also known as the data association problem [Montemerlo and Thrun \(2003\)](#) and many more.

Although the amount of research might seem overwhelming at first view, all current SLAM methodologies are founded on a single principle; the uncertainty of the map is correlated through the agent's measurements. When an agent localises itself (by reducing position uncertainty) all previously landmarks have their uncertainty reduced since the uncertainty is correlated with that of the agent's uncertainty.

There are three main paradigms to solving the SLAM problem. The first is EKF-SLAM (Extended-Kalman Filter) [Durrant-Whyte and Bailey \(2006\)](#). EKF-SLAM models the full state, being the agent's parameters and environmental features, by a Multivariate Gaussian distribution. The uncertainty of each individual feature is parametrised by a mean (expected position of the feature) and covariance (how much uncertainty there is about the position of the feature).

The second approach is Graph-SLAM [Grisetti et al. \(2010\)](#). Graph-SLAM estimates the full path of the agent and considers every measurement to be a constraint on the agent's path. It is parameterised by the canonical Multivariate Gaussian. At each time step a new row and column is added to the precision matrix which encodes landmarks which have been observed as constraints on the robot's position. At predetermined times, a nonlinear sparse optimisation is solved to minimise all the accumulated constraints on the robot's path.

The third method is FastSLAM [Montemerlo et al. \(2003\)](#). FastSLAM exploits the fact that if we know the position of the agent with certainty all landmarks become independent. It models the distribution of the agent's position by a particle filter. Each particle has its own copy of the map and updates all landmarks independently which is the strength of this method. However, if many particles are required each must have its own copy of the map. It is beyond the scope of this chapter to provide a detailed review of these three paradigms and the reader is referred to [Sebastian Thrun and Fox \(2005\)](#), [Thrun and Leonard \(2008\)](#).

5.2.2 ACTIVE-SLAM & EXPLORATION

Active-SLAM refers to a decision theoretic process of choosing control actions so as to actively increase the convergence of the map. It is used in conjunction with exploration of an unknown environment in a SLAM setting. The two steps of this process are: (i) generate a set of candidate destination positions, (ii) evaluate these positions based on a utility function. The utility is a trade off between reducing the uncertainty of the map or reducing the uncertainty of the agent's position.

Most approaches use a two-level representation of the map in an exploration setting. At the lower level there is the chosen (landmark-based) SLAM filter and at the higher level a coarser representation of the world. Such representations can be occupancy grids [Thrun and Bü \(1996\)](#) which encode either occupied and free space or a topological representation [Kollar and Roy \(2008\)](#).

Early and current approaches to selecting candidate exploratory locations are based on evaluating Next-best-view [González-Baños and Latombe \(2002\)](#) locations. Next-best-view points are sampled around *free edges* which are at the horizon of the known map (*frontier* regions). In such a setting only target points are generated, not the full trajectory. Probabilistic Road Map (PRM) [Kavraki et al. \(1996\)](#) based methods have been used as planners to reach desired target locations, such as in [Huang and Gupta \(2008\)](#), where a Rapidly Exploring Random Trees (RRT) is combined with FastSLAM. In [Valencia et al. \(2012\)](#), paths to *frontier* regions are computed via PRM on a occupancy grid map and at the lower level they use Pose-SLAM (synonym for Graph-SLAM).

An alternative approach taken to generating candidate locations is the specification of high level macro actions, they being either *exploratory* or *revisiting* actions as is the case in [Stachniss et al. \(2005\)](#). Macro actions reduce the costly evaluation of actions, especially in the case of FastSLAM, which requires propagating the filter forward in time so as to infer the information gain of each action.

The last approach is to solve the planning problem through formulating it as Partially Observable Markov Decision Process (POMDP) [Ross et al. \(2008\)](#). However all methods take an approximation of the POMDP and consider a one time step planning horizon ([Lidoris, 2011](#), p.37).

There are many ways of generating actions or paths, however their utility is nearly all exclusively based on the *information gain*, which is the estimated reduction of entropy a particular action or path would achieve. A few utilities use f-measures such as the Kullback-Leibler divergence. Evaluation of different utility metrics are presented in [Carrillo et al. \(2012\)](#); [Tovar et al. \(2006\)](#); [Carlone et al. \(2010\)](#).

5.3 Bayesian State Space Estimation

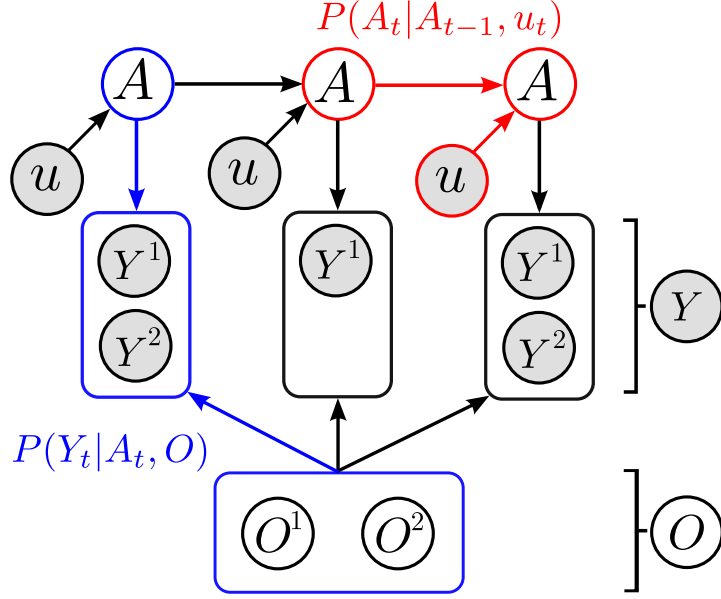


Figure 5.3: Directed graphical model of dependencies between the agent (A), sensing (Y) and action (u) random variables. Each object, $O^{(i)}$ is associated with one sensing random variable $Y^{(i)}$. The overall sensing random variable is $Y = [Y^{(1)}, \dots, Y^{(M-1)}]^T$, where M is the total number of agent and object random variables in the filter. For readability we have left out the time index t from A and Y . Since the objects are static, they have no temporal process associated with them thus they will never have a time subscript. The two models necessary for filtering are the motion model $P(A_t | A_{t-1}, u_t)$ (red) and measurement model $P(Y_t | A_t, O)$ (blue).

Bayesian State Space Estimation (BSSE) focuses on incorporating observations to update a prior distribution over the state space to a posterior distribution through the application of Bayes probability rules. The agent's random variable, A , is associated with the uncertainty of its location in the world, the same holds for the object(s') random variable(s), O . Given a sequence of actions and observations, $\{u_{1:t}, y_{0:t}\}$ (subscript $0 : t$ is the set from the time $t = 0$ to the current time, $t = t$), algorithms of the BSSE family incorporate this information to provide an estimate:

$$P(A_t, O | Y_{0:t}, u_{1:t}) \quad (5.3.1)$$

This is known as the filtering problem where all past information is incorporated to estimate the current state.

In Figure 5.3 we depict the general Bayesian Network (BN) of a BSSE. The BN conveys two types of information, the dependence and independence relations between the random variables in the graph which can be established through *d-separation* [Shachter \(1998\)](#), see Figure 5.4. Any joint probability distribution whose factorisation respects the structure of a BN is guaranteed to satisfy all the conditional independence statements which can be read from

Dependence & Independence

Conditional independence

- | | |
|---|---|
| 1) $A_{t+1} \perp\!\!\!\perp A_{t-1} A_t$ | First order Markov property. |
| 2) $A_t \perp\!\!\!\perp Y_{t+1} A_{t+1}$ | Past states do not depend on future observations. |
| 3) $A \perp\!\!\!\perp O \emptyset$ | Agent and object random variables are independent given no observation. |

Conditional dependence

- | | |
|-----------------------------------|--|
| 1) $A \not\perp\!\!\!\perp O Y$ | Agent and object random variables will interact with each other given an observation |
|-----------------------------------|--|

Figure 5.4: Dependence and independence relation between the random variables of the BN Figure 5.3

the graph, but the converse with respect to the dependence statements is not guaranteed (Barber, 2012, p.43).

The **conditional dependence** $A \not\perp\!\!\!\perp O | Y$ is key to all BSSE and SLAM algorithms. The strength of the dependence between the agent and object random variable is governed by the measurement likelihood $P(Y_t | A_t, O)$. If it does not change the joint distribution then the agent and object random variables will be independent, $A \perp\!\!\!\perp O$. If they are independent, then no information acquired by the agent can be used to infer changes in the object estimates.

We next demonstrate the behaviour of the two different parameterisations of the joint distribution of the BN, Figure 5.3, in the case of the absence of direct sighting of the object by the agent. We first consider a Multivariate Gaussian parameterisation of the joint distribution, which is known as EKF-SLAM, and a different approach which discretises the joint distribution, called Histogram-SLAM.

EKF-SLAM

In EKF-SLAM the joint density $p(A_t, O | Y_{0:t}, u_{1:t}) = g(x; \mu_t, \Sigma_t)$ is parametrised by a single Gaussian function g with mean, $\mu_t = [\mu_{A_t}, \mu_{O^{(1)}}, \dots, \mu_{O^{(M-1)}}]^T \in \mathbb{R}^{3+2 \cdot (M-1)}$ where the random variables are in \mathbb{R}^2 , and covariance, Σ_t . The mean value of the agent $\mu_a = [x, y, \phi]^T \in \mathbb{R}^3$ and those of the objects are $\mu_{O^{(i)}} = [x, y]^T \in \mathbb{R}^2$.

$$\Sigma_t = \begin{bmatrix} \Sigma_a & \Sigma_{ao} \\ \Sigma_{oa} & \Sigma_o \end{bmatrix} \in \mathbb{R}^{(3+2 \cdot (M-1)) \times (3+2 \cdot (M-1))} \quad (5.3.2)$$

The j 'th object measurement is described by range and bearing $Y_t^{(j)} = [r, \phi]$ in the frame of reference of the agent, see Figure 2.4 page 19 for an illustration of a measurement update process. EKF-SLAM assumes that the measurement

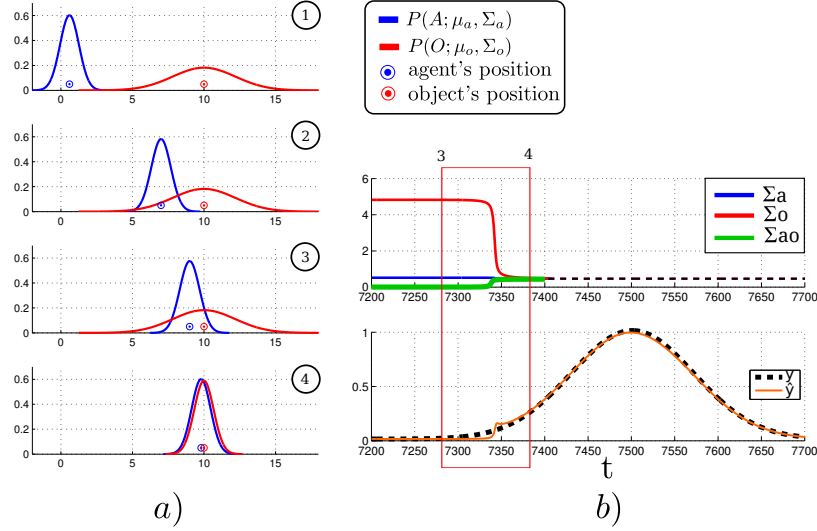


Figure 5.5: **a)** EKF-SLAM time slice evolutions of the pdfs. The temporal ordering is given by the numbers in the top right corner of each plot. The blue pdf represents the agent's believed location and the circle is the agent's true location. The same holds for the red distribution which represents the agent's belief of the location of an object. **b)** Evolution of the covariance components of Σ over time and true Y_t and expected measurements, \hat{Y}_t . Σ_a and Σ_o are the variances of the agent and object positions and Σ_{ao} is the cross-covariance term.

is corrupted by Gaussian noise, $\epsilon \sim \mathcal{N}(0, R)$, and this results in a measured likelihood function of the following form:

$$p(Y_t|A_t, O_t) = \frac{1}{|2\pi R|^{\frac{1}{2}}} \exp\left(-\frac{1}{2}(Y_t - \hat{Y}_t)^T R^{-1}(Y_t - \hat{Y}_t)\right) \quad (5.3.3)$$

$$\hat{Y}_t = \exp\left(-\frac{1}{2\sigma^2} \|A_t - O\|^2\right) \quad (5.3.4)$$

where the covariance, R , encompasses the uncertainty in the measurement and Equation 5.3.4 is the measurement function. The elements of the covariance matrix capture the measurement error between the true Y and expected \hat{Y} range and bearing of the object. As the joint distribution is parametrised by a single Multivariate Gaussian, a closed form solution to the filtering Equations exists, called the Kalman Filter [Durrant-Whyte and Bailey \(2006\)](#).

The error between the true and expected measurement $e = (Y_t - \hat{Y}_t)$ is an important part of the application of EKF-SLAM. In our scenario the agent can only perceive the objects once he enters in direct contact with them. This means that the variance of the observation Y_t will be very low and will always be equal to \hat{Y} until a contact occurs. To illustrate the problems which this gives rise to, we give an illustration of a 1D search. Figure 5.5 shows the resulting updates of the beliefs for 4 chosen time segments.

As expected we do not get the desired behaviour, which is that the beliefs start updating as soon as they are overlapping, see 2nd-3rd temporal snapshot in the Figure. Even when most of the belief mass of the agent's location pdf over-

laps that of the object pdf, no belief update occurs. The multivariate Gaussian parameterisation only guarantees a dependency between the agent and object random variables when there is a positive sighting of the landmarks. This can be seen in Figure 5.5 (b), where the component Σ_{ao} is 0 most of the time which implies that $A \perp\!\!\!\perp O|Y$ which is undesirable. This confirms that the dependencies present in the structure given by the BN are dependent on the chosen parametrisation.

HISTOGRAM-SLAM

In Histogram-SLAM, the joint distribution is discretized and each bin has a parameter, $P(A_t = i, O = j|Y_{0:t}, u_{1:t}) = \theta^{(ij)}$, which sums to one, $\sum_{ij} \theta^{(ij)} = 1$. For shorthand notation we will write $P(A_t, O|Y_{0:t}, u_{1:t})$ instead of $P(A_t = i, O = j|Y_{0:t}, u_{1:t})$. The probability distribution of the agent's position is given by marginalising the object random variable:

$$P(A_t|Y_{0:t}, u_{1:t}) = \sum_{j=1}^{|O|} P(A_t, O|Y_{0:t}, u_{1:t}) \quad (5.3.5)$$

$$P(A_t = 1|Y_{0:t}, u_{1:t}) = \sum_{j=1}^{|O|} \theta^{(1j)} \quad (5.3.6)$$

The convex polytope holds true for the object's marginal over its believed position. Figure 5.6 illustrates the joint distribution of both the agent and the object random variable. For ease of notation we use the shorthand $P(\theta)$ or $P(A_t|Y_{0:t}, u_{1:t})$. The 1D world of the agent and object is discretised to 10 states, producing a joint distribution with 100 parameters! For a state space of N bins, $i = 1 \dots N$, and there is a total of M random variables (one agent and $M - 1$ objects) and the joint distribution has N^M parameters. This exponential increase renders Histogram-SLAM intractable with this parameterisation.

Histogram likelihood model

A measurement model, $P(Y_t|A_t, O)$, predicts the likelihood of observations, Y_t , given the state of A_t and O . In the tasks we consider, an observation occurs only if the agent enters in contact with the object, which implies that both occupy the same discrete state.

$$P(Y_t = 1|A_t, O) = \begin{cases} 1 & \text{if } A_t = O \\ 0 & \text{if } A_t \neq O \end{cases} \quad (5.3.7)$$

Figure 5.7, illustrates the likelihood of Equation 5.3.7 in the case when a no contact measurement $Y_t = 0$ is present in a 1D world. Both likelihoods are sparse in the sense that there is only a small region which gets affected by the likelihood. When there is no measurement (*Left*) all the parameters of the joint

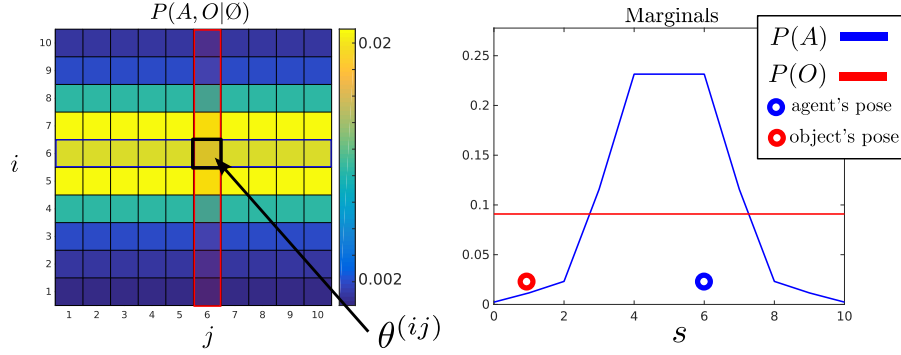


Figure 5.6: *Left:* Joint distribution of the agent and object before any action or measurement is initiated. *Right:* Marginals of the agent and object, giving the probability of their location. The marginal of each random variable is obtained from Equation 5.3.5. The probability of the agent and object being in state $s = 6$ is given by summing the blue and red highlighted parameters from the joint distribution.

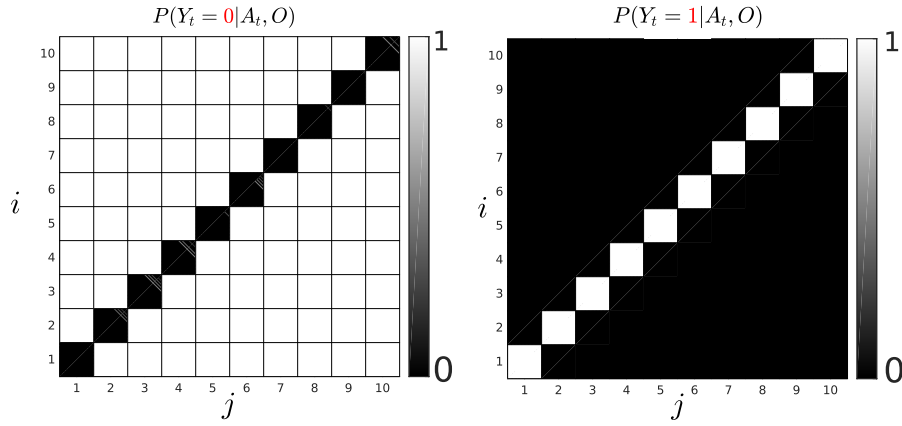


Figure 5.7: 1D world Likelihood $P(Y_t|A_t, O)$. *Left:* No contact detected with the object, the current measurement is $\hat{Y}_t = 0$, both the agent and object cannot be in the same state. *Right:* The agent entered into contact with the object and received a haptic feedback $Y_t = 1$. There are only two measurements contact or no contact, which the agent receives.

distribution which are in the black regions will become zero. When the object is detected (*Right*) then only parameters of the joint distribution which are within the white regions will be non-zero. All changes to the joint distribution are constrained to the states $i = j$, which in the case of a 2-dimensional joint distribution is a line. The **sparsity** of the likelihood function will be key to the development of the MLMF filter.

Two models are needed to perform the recursion, namely the motion model $P(A_t|A_{t-1}, u_t)$ and the measurement model $P(Y_t|A_t, O)$, which we already detailed. Both models applied consecutively to the initial joint distribution results in a posterior distribution. Both Equation 5.3.9-5.3.10 are part of the histogram Bayesian filter update:

Discrete Bayesian filter recursion

intialisation

$$P(A_0, O) = P(A_0)P(O) = \theta^{(i)}\theta^{(j)} = \theta^{(i,j)} \quad (5.3.8)$$

motion

$$P(A_t, O|Y_{0:t-1}, u_{1:t}) = \sum_{A_{t-1}} P(A_t|A_{t-1}, u_t)P(A_{t-1}, O_t|Y_{0:t-1}, u_{1:t-1}) \quad (5.3.9)$$

measurement

$$P(A_t, O|Y_{0:t}, u_{1:t}) = \frac{P(Y_t|A_t, O)P(A_t, O|Y_{0:t-1}, u_t)}{P(Y_t|Y_{0:t-1})} \quad (5.3.10)$$



For the derivation of these two steps, the reader is referred to Appendix 5.7.1. Figure 5.8 illustrates how the joint distribution evolves in a 1D world. The agent and object's true positions (unobservable) are in state 6 and 1. The agent moves four steps towards state 10. At each time step, as the agent does not sense the object, the likelihood function $P(Y_t = 0|A_t, O)$ (Figure 5.7 Left) is applied. As the agent moves towards the right, the motion model shifts the joint distribution towards state 10 along the agent's dimension, i (note that state 1 and 10 are wrapped).

As the agent moves to the right more joint distribution parameters become zero and the re-normalisation by the **evidence** ($P(Y_t|Y_{0:t-1})$, denominator of Equation 5.3.10), which increases the value of the remaining parameters, is equal to the sum of the probability mass which was set to zero by the likelihood function. Thus the values of the parameters of the joint distribution which fall on the pink line in Figure 5.8 (green line also, but only for first time slice) become zero and their values are redistributed to the remaining non-zero parameters. This is an **important aspect** which will be present in MLMF and we define this to be $\alpha \in \mathbb{R}$.

When the agent enters into contact with the object and senses it, the likelihood function $P(Y_t = 1|A_t, O)$, Figure 5.7 (Right), is multiplied with the joint distribution with the result illustrated in Figure 5.9. Only parameters of the joint distribution whose indices satisfy $i = j$ will remain unchanged, all the others will become zero. In retrospect the likelihood $P(Y_t = 1|A_t, O)$ acts as a **constraint**, that is, the agent and object have to be in the same state given by a line traversing the 2D joint distribution.

The **inconvenience** with Histogram-SLAM is that its time and space complexity is exponential, as the joint distribution is discretized and parametrised by $\theta^{(ij)}$. Instead we propose a filter, named MLMF, which does not parameterise the joint distribution.

The particularity of the new filter, MLMF, which we formally introduce in the next section, is to achieve the same result as the Histogram filter but without having to parameterise the joint distribution, thus avoiding the exponential

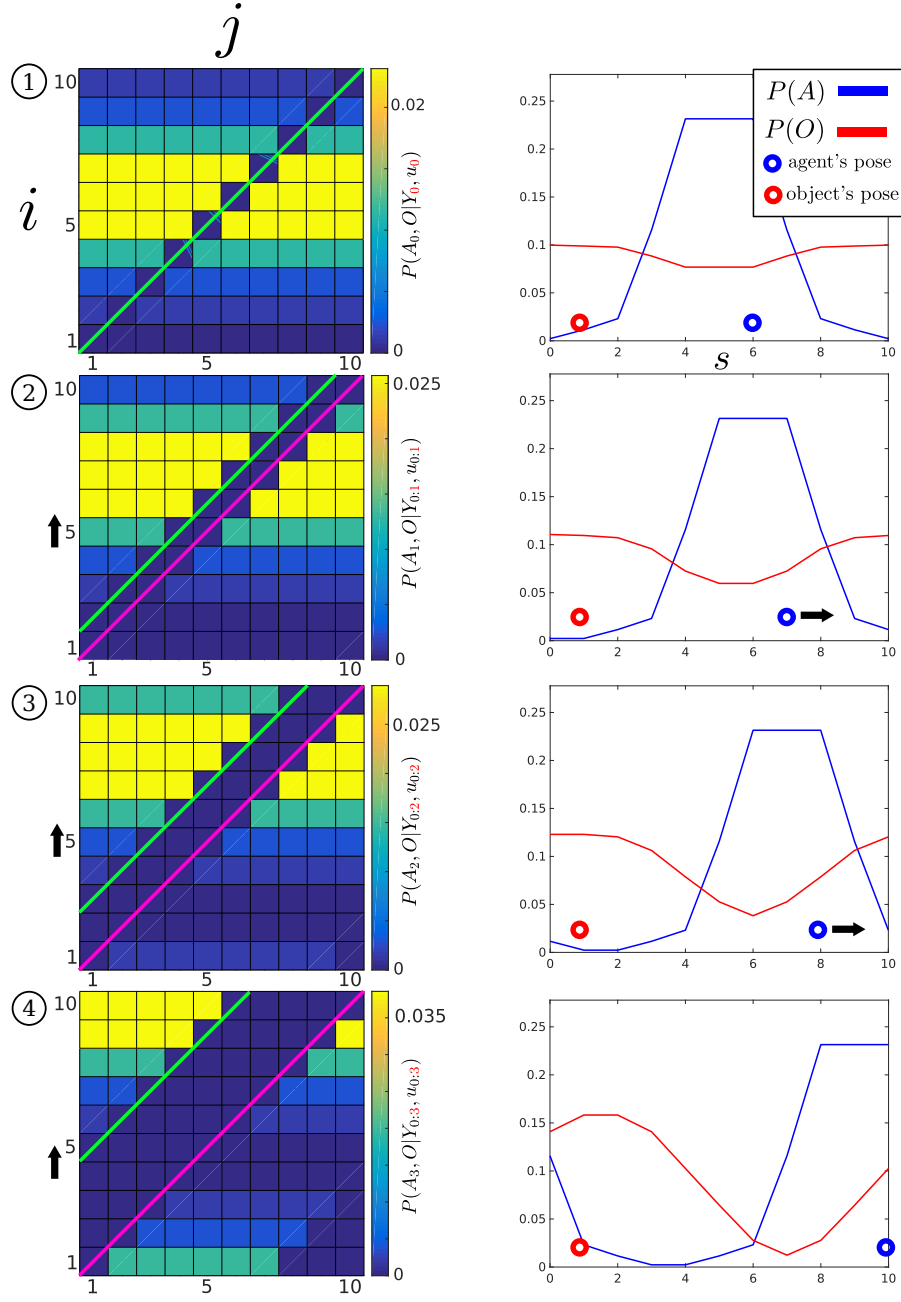


Figure 5.8: Histogram-SLAM, 4 time steps. **1** Application of likelihood $P(Y_0 = 0|A_0, O)$ and the agent remains stationary, $u_0 = 0$, all states along the green line become zero. **2** The agent moves to the right $u_1 = 1$, the motion $P(A_1|A_0, u_1)$, and likelihood models are applied consecutively. The right motion results in a shift (black arrow on the left) in the joint probability distribution towards the state $i = 10$. All parameters on the pink line are zero. **3** Same as two. **4** The original result of the likelihood function, green line, has moved by the same amount as the agent's displacement. At each time step a new likelihood function (pink line) is applied to the joint distribution.

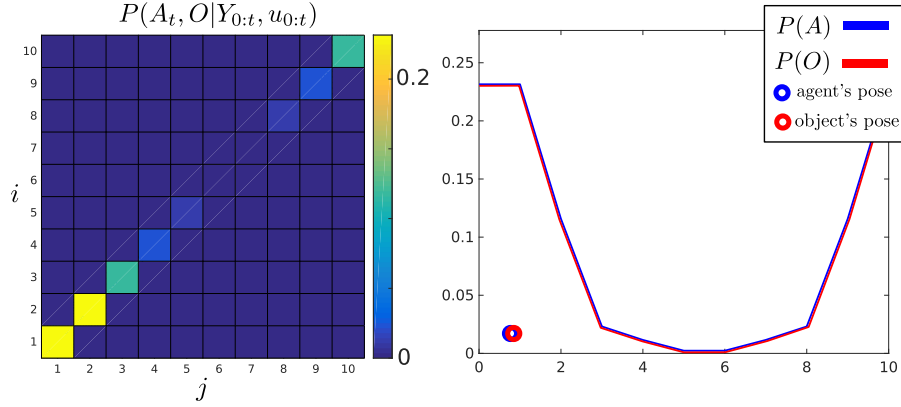


Figure 5.9: Histogram-SLAM contact. The agent has entered in contact with the object (measurement $Y_t = 1$) and the likelihood function $P(Y_t = 1 | A_t, O)$ is applied to the joint distribution. Only parameters on the line $i = j$ will remain unchanged and parameters for which $i \neq j$ will be set to zero.

growth cost. The **key idea** behind the mechanism of the MLMF filter is to only evaluate the joint distribution in states (i, j) for which the likelihood is zero and apply the updates directly to the marginals without parameterising the values of the joint distribution. The MLMF filter parametrises **explicitly** the marginals $P(A_t = s | Y_{0:t}, u_{1:t}) : \theta_a^{(s)}$, $P(O = s | Y_{0:t}, u_{1:t}) : \theta_o^{(s)}$. This is in contrast to the Histogram filter in which the marginals are derived from the joint distribution by marginalisation. For the MLMF filter, in order to respect the Bayesian recursion, the filter has to **memorise** the complete history of likelihood functions $\{P(Y_t | A_t, O)\}_{t=0:T}$ and the normalisation coefficient α . The reasons for this will be made clear in the next section. Below we summarise the parameters of the Histogram and the desired MLMF parameters:

Histogram	: $\theta^{(ij)}$
desired-MLMF	: $\theta_a^{(s)}, \theta_o^{(s)}, \alpha, \{(Y, l)_p\}_{p=0:t}$ $s, i, j = 1, \dots, N$

The likelihood function is parametrised by a measurement, Y_t and offset l to the i -axis. In Figure 5.8 we see that the likelihood applied at the first time step (green line) is superimposed on the line $i = j$. As actions are applied, $u_{1:3} = [1, 1, 1, 1]$, the first likelihood function (green line) shifts by an amount corresponding to the total displacement (4 in this case), see the last sub-figure of 5.8. The second likelihood applied at $t = 1$ will have an offset corresponding to the sum $u_{1:3}$, the third will have an offset of $u_{2:3}$ and so on and so forth.

The MLMF, which we mathematically derive in the next section, keeps as parameters the marginals, likelihood function parameters and a normalisation constant. The marginals are updated (filter recursion) by **evaluating** the joint distribution in states which are set to zero by the current applied likelihood and removing the value of the zeroed parameters from the marginals.

When a positive contact is established with the object, the likelihood is

zero everywhere other than the states corresponding to $i = j$, see Figure 5.9. In this case there is no need to evaluate the likelihood elsewhere in the joint distribution. The marginals are simply the normalisation of the line $i = j$. The evaluation of the joint distribution, given that the object is sensed or not, is restricted to the states (i, j) for which $i = j$ and there are a total of N states. This is much less than N^2 which Histogram-SLAM requires.

5.4 Measurement Likelihood Memory Filter

To obtain an informative update of the marginals, the random variables A and O must remain dependent in the absence of a positive observation Y . Additionally, this dependence should be efficiently encoded in contrast to the histogram parametrisation shown in Section 5.3.

The likelihood function $P(Y_t|A_t, O)$ is the cause of the dependence between the random variables. If both the agent and object were completely independent, no additional parameters would be required to represent the joint distribution other than the marginals $P(A_t)$ and $P(O)$ giving a total of NM parameters (where N is the number of states and M is the number of random variables). At the other extreme if every single point in the domain of the random variables was dependent this would require the totality of N^M parameters as previously stated in the case of the histogram filter. We propose a method in which we do not model the joint distribution explicitly but rather only compute its impact on the marginals.

5.4.1 MLMF PARAMETRISATION

The concept behind MLMF is to keep a **function parameterisation** of the joint distribution instead of a **value parameterisation** as it is the case for Histogram-SLAM. At initialisation the joint distribution is represented by the product of marginals, Equation 5.4.1, which would result in the joint distribution illustrated in Figure 5.6, if it were to be evaluated at all states (i, j) as it is done for Histogram-SLAM, Equation 5.3.8. MLMF will only evaluate this product at specific states, only when necessary. At each time step the motion and measurement update are applied, Equation 5.4.2-5.4.2. An important distinction is that these updates are performed on the joint distribution, which is not the case in Histogram-SLAM where the updates are done on the conditional, Equation 5.3.9-5.3.10. After applying multiple motion and measurement updates the resulting joint distribution is given by Equation 5.4.4, see Appendix 5.7.2 for a step-by-step derivation. The filtered condition, Equation 5.4.5, is the result of the normalisation of the filtered joint by the marginal likelihood.

MLMF Bayesian filter

initialisation

$$P(A_0, O) = P(A_0)P(O) \quad (5.4.1)$$

motion

$$P(A_t, O, Y_{0:t-1} | u_{1:t}) = \sum_{A_{t-1}} P(A_t | A_{t-1}, u_t) P(A_{t-1}, O, Y_{0:t-1} | u_{1:t-1}) \quad (5.4.2)$$

measurement

$$P(A_t, O, Y_{0:t} | u_{1:t}) = P(Y_t | A_t, O) P(A_t, O, Y_{0:t-1} | u_{1:t-1}) \quad (5.4.3)$$

filter (joint)

$$P(A_t, O, Y_{0:t} | u_{1:t}) = P(O) P(A_t | u_{1:t}) \prod_{i=1}^t P(Y_i | A_t, O) \quad (5.4.4)$$

filter (conditional)

$$P(A_t, O | Y_{0:t}, u_{1:t}) = \frac{P(A_t, O, Y_{0:t} | u_{1:t})}{P(Y_{0:t} | u_{1:t})} \quad (5.4.5)$$

The motion update, Equation 5.4.2, when applied to the joint distribution results in the initial marginal $P(A_t)$ and the likelihood functions being moved along the agent's axis. Equation 5.4.5, would require an expensive evaluation of Equation 5.4.4 at each state (i, j) resulting in the evaluation of the likelihood product. We will demonstrate that MLMF only evaluates dependent states (i, j) (states which are affected by the likelihood at the current time step). The MLMF filter is parameterised by the agent and object marginals $P(A_t | u_{1:t})$, $P(O)$ and the history of likelihood functions, Equation 5.4.4, which is all the likelihood functions since $t = 0$ until t :

$$P(Y_{0:t} | A_t, O; \Psi_t) := \prod_{i=0}^t P(Y_i | A_t, O) \quad (5.4.6)$$

The likelihood functions have two different functional forms (see Figure 5.7) which is dictated by the current binary measurement and the offset of the likelihood function along the agent's axis. The parameters of Equation 5.4.6 are all the measurements since the start of the filtering and offsets along the agent's axis, we refer to these parameters as $\Psi_t = \{(Y_{p=0:t}, \text{offset})\}$. In Algorithm 1, we detail how a measurement and action at time step t , result in the update of the likelihood functions; this is an implementation of Equation 5.4.2 for the likelihood product.

Algorithm 1: Likelihood functions update

input : Ψ_{t-1}, Y_t, u_t

output: Ψ_t

```
1 motion update
2 for  $l_{t-1} \in \Psi_{t-1}$  do
3    $l_t = l_{t-1} + u_t$ 
4 measurement update
5  $\Psi_t \leftarrow \{\Psi_{t-1}, (Y_t, l = 0)\}$ 
```

Figure 5.10 illustrates the evolution of the MLMF joint distribution, Equation 5.4.5, for two actions and three measurements. On the *left* a green line passes through the probability mass of the joint distribution which was initialised to $P(A_0, O) = P(A_0)P(O)$. The states (i, j) in the joint distribution on the green line are evaluated to zero by the likelihood function $P(Y_0 = 0|A_t, O)$, since no object was sensed. As the agent takes two actions towards state 100 the original marginal distribution of the agent, $P(A_0)$, is updated according to Equation 5.4.2 as are the likelihood functions, resulting in $P(A_2|u_{1:2})$, $P(Y_0|A_2, O)$ and $P(Y_1|A_2, O)$. The likelihood function $P(Y_0|A_2, O)$ evaluates all states $(i + 2 = j)$ to zero and the likelihood $P(Y_1|A_2, O)$ evaluates states $(i + 1 = j)$ to zero. A new measurement is sensed and the corresponding likelihood function $P(Y_2|A_2, O)$ is added to the product of likelihoods, Equation 5.4.3, which evaluates all states (i, j) to zero. The parameters of Equation 5.4.6 will now be: $\Psi_2 = \{(0, 2)_{p=0}, (0, 1)_{p=1}, (0, 0)_{p=2}\}$. The probability mass which has been evaluated to zero is re-normalised to the remaining non-zero parameters of the joint distribution, as the joint distribution must sum to one.

For ease of notation from this point onwards we will not show the conditioned actions $u_{1:t}$, so $P(A_t, O|Y_{0:t}, u_{1:t})$ will be $P(A_t, O|Y_{0:t})$.

Our goal is to be able to compute the marginals $P(A_t|Y_{0:t})$, $P(O|Y_{0:t})$ of the agent and object random variables and marginal likelihood $P(Y_{0:t}|u_{1:t})$ **without** having to perform an **expensive marginalisation** over the entire space of the joint distribution as was the case for Histogram-SLAM.

The next section describes how to efficiently compute the normalisation factor, denominator Equation 5.4.5, and the marginals.

5.4.2 COMPUTATION OF EVIDENCE AND MARGINALS

In order to compute efficiently the marginal likelihood (also known as evidence) $P(Y_{0:t}|u_{1:t})$ and the filtered marginals $P(A_t|Y_{0:t})$, $P(O|Y_{0:t})$ we take advantage of the fact that only a very small area in the joint distribution space will be affected by the measurement likelihood function at each time step.

Without loss of generality the likelihood function will only make a difference to dependent $A \cap O$ regions in the joint distribution, areas where the likelihood

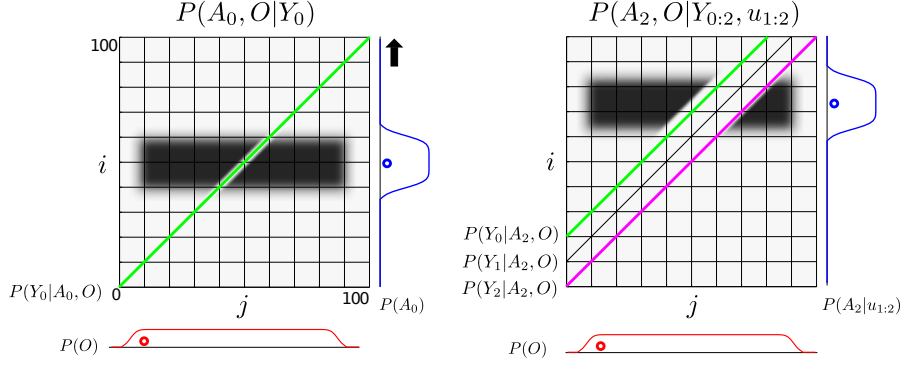


Figure 5.10: Evolution of the MLMF joint distribution (evaluation of Equation 5.4.5) and marginals for a 1D world. The space is discretised to 100 bins and the agent is moving in the direction of the black arrow. The black line correspond to areas in which the likelihood function evaluates to zero. *Left:* the first likelihood function $P(Y_0|A_0, O)$, causes all the mass of joint distribution whose's states are $i = j$ to be evaluated to zero, as the agent has not sensed the object (the red and blue circles on the marginals indicate the true position of both the agent and the object). The probability mass which lies in the area of influence of the measurement likelihood (evaluated to zero) gets removed and redistributed to the other states in the joint distribution due to normalisation. *Right:* Two actions have been taken and three measurements have been observed. The joint distribution on the *right* is the result of applying the motion update, Equation 5.4.2, which moves the initial marginal $P(A_0)$ to $P(A_2|u_{1:2})$ and displaces the likelihood function. A new measurement is then added, Equation 5.4.4, illustrated by the pink line.

function is less than one. The region inside $A \ominus O$ will not be affected, where the likelihood function is equal to one. Figure 5.11 shows the relation between the measurement function $P(Y_t|A_t, O)$ and the joint distribution $P(A_t, O|Y_{0:t})$ for three different initialisations.

As illustrated and explained in Figure 5.11, the joint distribution can be decomposed in a dependent and independent term (Equation 5.4.7).

$$P(A_t, O|Y_{0:t}) = P_{\cap}(A_t, O|Y_{0:t}) + P_{\ominus}(A_t, O|Y_{0:t}) \quad (5.4.7)$$

The probability mass covered by the dependent term is located within the measurement function's tube and the independent probability mass is located outside as shown in Figure 5.11. This formulation will lead to large computational gain as the independent term is not influenced by the measurement function: $P_{\ominus}(A_t, O|Y_{0:t}) \propto P_{\ominus}(A_t, O|Y_{0:t-1})$.

Evidence

The evidence of the measurement $P(Y_{0:t}|u_{1:t})$ is the normalisation coefficient of the joint distribution Equation 5.4.5. It is the amount of probability mass re-normalised to the other parameters as a result of the consecutive application of the likelihood function. At time step t , the normalising factor to be added to the evidence is the difference between the probability mass located inside $A \cap O$ before and after the application of the measurement function $P(Y_t|A_t, O)$, see

$$P(A_t, O|Y_{0:t}) = P_{\cap}(A_t, O|Y_{0:t}) + P_{\ominus}(A_t, O|Y_{0:t})$$

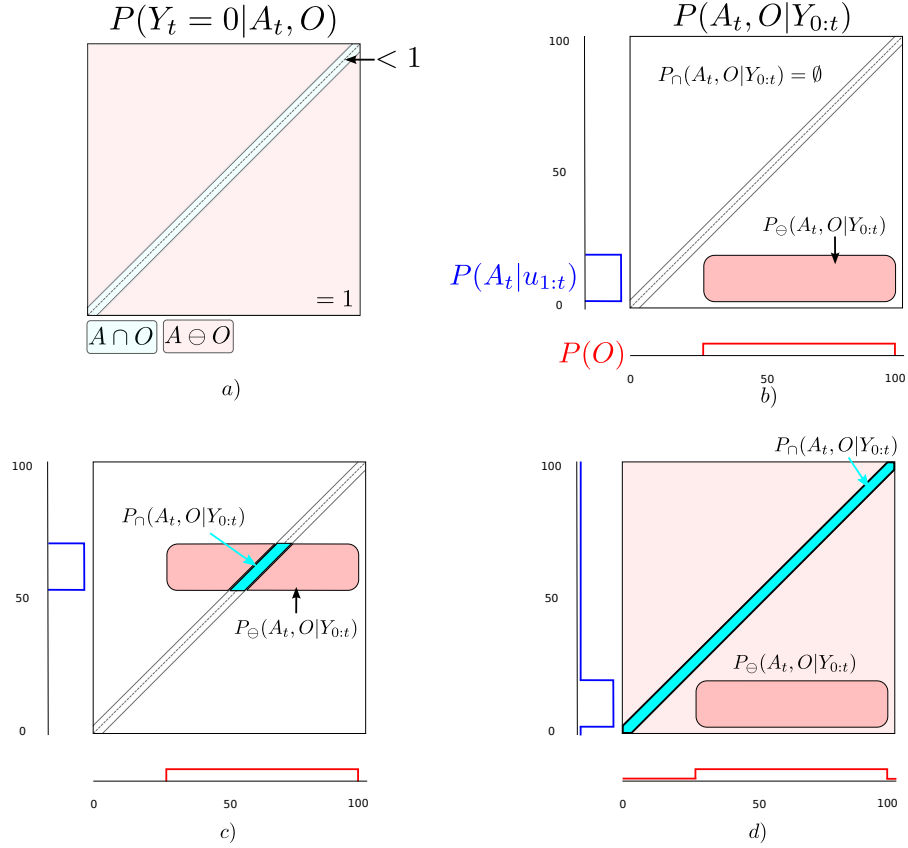


Figure 5.11: **a)** Likelihood $P(Y_t = 0|A_t, O)$, the blue area depicts the regions in which the likelihood is < 1 and the red area is where the likelihood is $= 1$. If the probability mass of the joint distribution is in the blue region, then the parameters of the random variables in these areas are dependent, $A \cap O$ and otherwise they are independent from one another, $A \ominus O$. **b)** The agent and object marginals are not overlapping and thus are completely independent. The joint distribution, $P(A_t, O|Y_{0:t})$ the black rectangle, is not intersecting with the measurement function. As a result $P_{\cap}(A_t, O|Y_{0:t})$ is empty. **c)** The marginals overlap resulting in the measurement likelihood function intersecting with the joint distribution. The joint distribution is composed of the blue and red areas, Equation 5.4.7. The probability mass at the intersection gets removed and re-normalised to other regions which is the result of applying Bayes integration. **d)** The marginals of A and O are completely overlapping, however only a small fraction of the probability mass in the joint distribution is within the measurement function's tube.

Equation 5.4.8 (see Appendix 5.7.3 for the full derivation).

$$P(Y_{0:t}|u_{1:t}) = 1 + \sum_{t=0}^t \left(\overbrace{\sum_{A_t} \sum_O (P(Y_t|A_t, O) - 1) P_{\cap}(A_t, O, Y_{0:t-1}|u_{0:t})}^{\alpha_t} \right) \quad (5.4.8)$$

The advantage of Equation 5.4.8 is that the summation is only over states which are in the dependent area \cap of the joint distribution. This is generally always much smaller than the full space itself. Until an object is sensed, the likelihood will always be zero $P(Y_t|A_t, O) = 0$ and α will correspond to the probability mass which falls within the region of the joint distribution in which the likelihood function is zero. In Figure 5.11 b) & d), the sum of the probability mass in the blue regions is equal to α . The point of interest is that as we perform the filtering process we will never re-normalise the whole joint distribution, but only keep track of how much it should have been normalised. To this end the marginals $P(A_t|u_{1:t})$ and $P(O)$ are never re-normalised but are used to compute at each step how much of the probability mass α_t should go to the normalisation factor $P(Y_{0:t}|u_{1:t})$. The evidence in question will never be negative, as the joint distribution sums to one and each α_t represents some of the mass removed from the joint distribution. Since we keep track of the history of applied measurement likelihood functions we never remove the same amount of probability mass twice from the joint distribution.

Marginals

There are two different types of marginals used in the MLMF filter. The first set are the initial **joint marginals** of the joint distribution, Equation 5.4.4. The second set of marginals are the **filtered marginals** which are updated by evaluating the joint distribution in dependent states.

Marginals

joint marginals

$P(A_t|u_{1:t})$ and $P(O)$: Equation 5.4.4

filtered marginals

$P(A_t|Y_{0:t}, u_{1:t})$ and $P(O|Y_{0:t})$

In Histogram-SLAM both the agent and object marginals are obtained, at every time, by marginalising the joint distribution. This requires storing and summing over all the parameters of the joint distribution which is expensive. Instead in MLMF we take advantage of the sparsity of the likelihood function and as a result we take only the dependent marginal components into consideration, Equation 5.4.9.

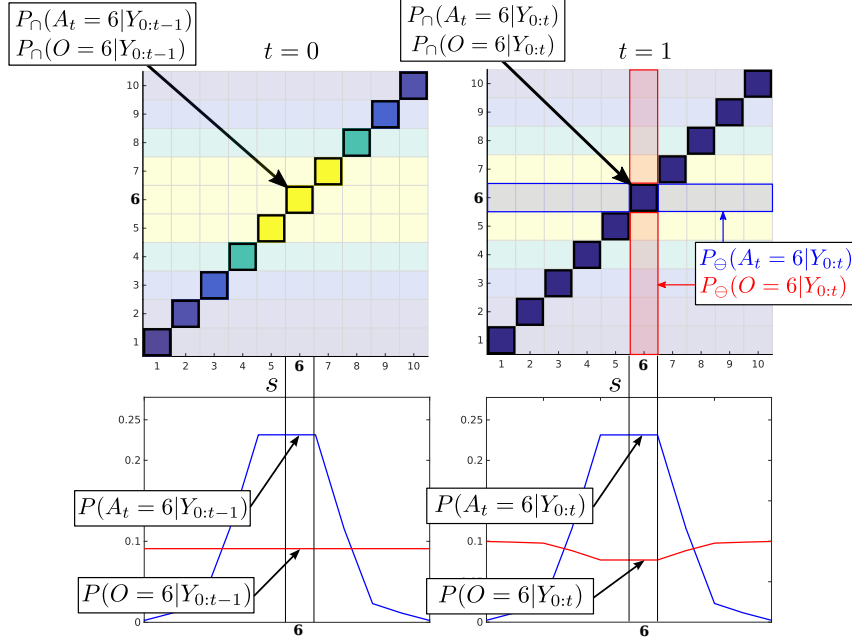


Figure 5.12: Filtered Marginals. Illustration of the agent and object marginal update, Equation 5.4.9. The parameters of the joint distribution which are independent $A \ominus O$ are pale and the dependent areas $A \cap O$, where $P(Y_t < 1 | A_t, O)$, are bright. MLMF only evaluates the joint distribution in dependent states. For each state s of the marginals $1, \dots, 10$ the difference of the marginals inside the dependent area, before and after the measurement likelihood is applied, is evaluated and removed from the marginals $P(A_t | Y_{0:t-1})$, $P(O | Y_{0:t-1})$ leading to $P(A_t | Y_{0:t})$, $P(O | Y_{0:t})$ (we did not show $u_{1:t}$ for easing the notation).

$$P(A_t | Y_{0:t}) = P(A_t | Y_{0:t-1}) - \left(P_{\cap}(A_t | Y_{0:t-1}) - P_{\cap}(\mathbf{A}_t | \mathbf{Y}_{0:t}) \right) \quad (5.4.9)$$

(see Appendix 5.7.4 for the full derivation of Equation 5.4.9).

$$P_{\cap}(\mathbf{A}_t | \mathbf{Y}_{0:t}) = \frac{\sum_O \overbrace{P(Y_t | A_t, O) P_{\cap}(A_t, O, Y_{0:t-1} | u_{1:t})}^{P_{\cap}(A_t, O, Y_{0:t} | u_{1:t})}}{1 - \underbrace{(\alpha_0 + \alpha_1 + \dots + \alpha_t)}_{P(Y_{0:t} | u_{1:t})}} \quad (5.4.10)$$

$$= \sum_O P_{\cap}(A_t, O | Y_{0:t}) \quad (5.4.11)$$

Equation 5.4.9 is recursive, $P(A_t, \text{yellow box})$ is computed in terms of $P(A_t, | Y_{0:t-1})$. In Figure 5.12 we illustrate how the MLMF updates the marginals of the agent and object given a new measurement. The illustrated marginals (*Bottom row*) are the **filtered marginals** $P(A_t | Y_{0:t}, u_{1:t})$, $P(O | Y_{0:t})$. The shape of the **joint marginals** $P(A_t | u_{1:t})$, $P(O)$ (not shown) will remain unchanged by measurements during the filtering process. They are the parameters of the joint distri-

bution used to update the filtered marginals.

Table 5.1 summarises the functions and parameters of the MLMF for two random variables, an agent and object.

functions	parameters	description
$P(A_t Y_{0:t}, u_{1:t})$	θ_a	filtered marginals
$P(O Y_{0:t})$	θ_o	
$P(A_t u_{1:t})$	θ_a^*	joint marginals
$P(O)$	θ_o^*	
$P(Y_{0:t} u_{1:t})$	$\alpha \in \mathbb{R}$	evidence
$P(Y_{0:t} A_t, O)$	$\Psi = \{(Y, l)_p\}_{p=0:t}$	likelihood history

Table 5.1: MLMF functions with associated parameters. The marginal parameters are the discretisation of the state space $\theta \in \mathbb{R}^N$, $\theta^{(s)}$ corresponds to the probability being in state s .

5.4.3 MLMF-SLAM ALGORITHM

Algorithm 2: MLMF-SLAM

input :

measurements

Y_t, u_t

joint functions:

$P(A_{t-1}|u_{1:t-1}) P(O), P(Y_{0:t-1}|A_{t-1}, O), \alpha_{0:t-1}$

filtered marginals:

$P(A_{t-1}|Y_{0:t-1}, u_{1:t-1}), P(O|Y_{0:t-1})$

output:

joint functions:

$P(A_t|u_{1:t}), P(Y_{0:t}|A_t, O), \alpha_{0:t}$

filtered marginals:

$P(A_t|Y_{0:t}, u_{1:t}), P(O|Y_{0:t})$

6 motion update

$$7 \quad P(A_t|u_{1:t}) = \sum_{A_{t-1}} P(A_t|A_{t-1}, u_t) P(A_{t-1}|u_{1:t-1})$$

$$8 \quad P(A_t|Y_{0:t}, u_{1:t}) = \sum_{A_{t-1}} P(A_t|A_{t-1}, u_t) P(A_{t-1}|Y_{0:t-1}, u_{1:t-1})$$

$$9 \quad P(Y_{0:t-1}|A_t, O) \leftarrow \text{motion update Algorithm 1}$$

10 measurement update

$$11 \quad P(A_t|Y_{0:t}) = P(A_t|Y_{0:t-1}) - (P_{\cap}(A_t|Y_{0:t-1}) - P_{\cap}(A_t|Y_{0:t}))$$

$$12 \quad P(O|Y_{0:t}) = P(O|Y_{0:t-1}) - (P_{\cap}(O_t|Y_{0:t-1}) - P_{\cap}(O_t|Y_{0:t}))$$

$$13 \quad \alpha_{0:t} = \alpha_{0:t-1} + \sum_{A_t} \sum_O P_{\cap}(A_t, O|Y_{0:t-1})(1 - P(Y_t|A_t, O))$$

$$14 \quad P(Y_{0:t}|A_{0:t}, O) \leftarrow \text{measurement update Algorithm 1}$$

In Algorithm 2 we detail the motion-measurement update steps of MLMF-SLAM. This formulation is advantageous as the joint distribution is only evaluated inside the dependent regions $A \cap O$ of the joint distribution. Through the term $P(Y_{0:t}|A_t, O)$ we keep track of the normalisation factor $P(Y_t|Y_{0:t-1})$ which is a scalar, and where we have previously applied the likelihood function.

We evaluated this formulation of the joint distribution with the standard histogram filter in the case of the 1D search routine illustrated in Figure 5.10 and we found them to be identical. Having respected the formulation of Bayes rule, we assert that Algorithm 2 is a Bayesian Optimal Filter. ¹.

5.4.4 SPACE & TIME COMPLEXITY

For discussion purposes we consider the case of three beliefs, namely that of the agent and two other objects $O^{(1)}$ and $O^{(2)}$ which we subsequently generalise. As stated previously M stands for the number of filtered random variables including the agent. N is the number of discrete states in the world. In the following section, we compare MLMF-SLAM with the Histogram-SLAM.

SPACE COMPLEXITY

Figure 5.13 *left* illustrates the volume occupied by the joint distribution for a marginal space of N states. Histogram-SLAM would require N^3 parameters for the joint distribution $P(A, O^{(1)}, O^{(2)})$ and N^M for M random variables.

For MLMF-SLAM, each random variable X requires two sets parameters θ and θ^* (see Table 5.1). Given M random variables, the initial number of parameters is $M(2N)$. At every time step the likelihood memory function increments by one measurement and offset, $(Y_t, l = 0)$ (Algorithm 1). Given a state space of size N , there can be no more than N different measurement functions (one for each state). In the worst case scenario the space complexity of the memory will be N , giving a total of $M(2N) + N$. The final worst case space complexity is linear in the number of random variables, $\mathcal{O}(NM)$.

TIME COMPLEXITY

For Histogram-SLAM, the computational cost is equivalent to that of the space complexity, $\mathcal{O}(N^M)$, since every state in the joint distribution has to be summed to obtain all the marginals.

For MLMF-SLAM, every state in the joint distribution's state space which has been changed by the measurement likelihood function has to be summed, see Figure 5.12. As a result the computational complexity is directly related

¹An optimal Bayesian solution is an exact solution to the recursive problem of calculating the exact posterior density Arulampalam et al. (2002b)

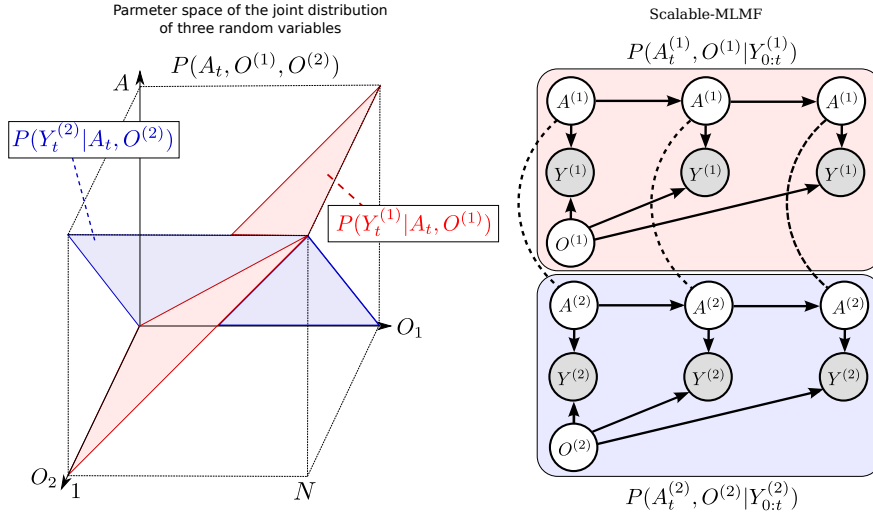



Figure 5.13: *Left:* Joint distribution $P(A, O^{(1)}, O^{(2)})$ of the agent and two objects. Each measurement likelihood function, $P(Y|A, O^{(1)})$, $P(Y|A, O^{(2)})$ corresponds to a hyperplane in the joint distribution. The state space is discretised to N bins giving the total number of parameters in the joint distribution of N^3 . *Right: Scalable-MLMF* Each agent-object joint distribution pair is modelled independently. For clarity we have left out the action random variable u which is linked to every agent node. Two joint distributions $P(A^{(1)}, O^{(1)}|Y_{0:t}^{(1)})$ and $P(A^{(2)}, O^{(2)}|Y_{0:t}^{(2)})$ parametrise the graphical model. The dashed undirected lines represent a wanted dependency, if present $O^{(1)}$ and $O^{(2)}$ are to be dependent through A . In the standard setting there will be no exchange of information between the individual joints. However we demonstrate later on how we perform a one time transfer of information when one of the objects is sensed.

to the number of dependent states $|A \cap O|$. In Figure 5.13 *left*, the number of effected states are shown by the blue and red planes. For M random variables the computational cost is $\mathcal{O}(N^{M-1})$ pposed to $\mathcal{O}(N^M)$. The computation complexity in this setup is still exponential but to the order $M - 1$ as opposed to M which will nevertheless quickly limit the scalability as more objects are added.

Computing the value of a dependent state (i, j) in the joint distribution required evaluating Equation 5.4.4 which contains a product of t likelihood functions. However the likelihood functions are not overlapping and binary. As a result complete product does not have to be evaluated since only one likelihood function will effect the state (i, j) . Thus evaluating Equation 5.4.4 yields a cost of $\mathcal{O}(1)$ and **not** $\mathcal{O}(t)$.

5.4.5 SCALABLE EXTENSION TO MULTIPLE OBJECTS

To make our filter scalable we introduce an **independence assumption** between the objects and model the joint distribution (Equation 5.4.12) as a product of agent-object joint distributions:

$$P(A_t, O^{(1)}, \dots, O^{(M-1)} | Y_{0:t}) = \prod_{i=1}^{M-1} P(A_t^{(i)}, O^{(i)} | Y_{0:t}^{(i)}) \quad (5.4.12)$$

The measurement variable Y_t , is the vector of all agent-object measurements, $Y_t = [Y_t^{(1)}, \dots, Y_t^{(M-1)}]^T$. Each agent-object joint distribution has its own parametrisation of the agent's marginal, $A_t^{(1)}, \dots, A_t^{(M-1)}$ which combine to give the overall marginal of the agent A_t .

The computation of each object marginal $P(O^{(i)} | Y_{0:t}^{(i)})$ is independent of the other objects. This is evident from the marginalisation see Equation 5.4.13-5.4.15.

$$P(O^{(i)} | Y_{0:t}^{(i)}) = \sum_{A_t^{(i)}} P(A_t^{(i)}, O^{(i)} | Y_{0:t}^{(i)}) \quad (5.4.13)$$

$$P(A_t | Y_{0:t}) = \prod_{i=1}^{M-1} \left(\sum_{O_i} P(A_t^{(i)}, O^{(i)} | Y_{0:t}^{(i)}) \right) \quad (5.4.14)$$

$$= \prod_{i=1}^{M-1} P(A_t^{(i)} | Y_{0:t}^{(i)}) \quad (5.4.15)$$

The independence assumption will create an unwanted effect with respect to agent's marginal $P(A_t | Y_{0:t})$. At initialisation the agent marginals should be equal, $P(A_0 | Y_0) = P(A_0^{(i)} | Y_0^{(i)}) \forall i$, however this is not the case because of Equation 5.4.15. To overcome this we define the final marginal, $P(A_t | Y_{0:t})$, of the agent as being the average of all the individual pairs $P(A^{(i)} | Y_{0:t}^{(i)})$.

$$P(A_t|Y_t) := \frac{1}{M-1} \sum_{i=1}^{M-1} P(A_t^{(i)}|Y_t^{(i)}) \quad (5.4.16)$$

Figure 5.13 (*Right*), depicts the graphical model of the scalable formulation. As each joint distribution pair has its own parametrisation of the agent's marginal and these do not subsequently get updated by one another, the information gained by one joint distribution pair is **not transferred**. A remedy is to transfer information between the marginals $A^{(i)}$ at specific intervals namely when one of the objects is sensed by the agent.

Algorithm 3: Scalable-MLMF: Measurement Update

```

input :  $P(A_t^{(i)}), P(A_t^{(i)}|Y_{0:t-1}^{(i)})$ 
          $P(O^{(i)}), P(O^{(i)}|Y_{0:t-1}^{(i)})$ 
          $Y_t^{(i)}$ 
          $i = 1, \dots, M$ 

  ▷ If object  $i$  has been sensed by the agent
15 if  $Y_t^{(i)} > 0$  then
16    $P(O^{(i)}|Y_{0:t}^{(i)}) \leftarrow P(O^{(i)}|Y_{0:t-1}^{(i)})$  ;    ▷ measurement update Algo. 2
17    $P(A_t^{(i)}|Y_{0:t}^{(i)}) \leftarrow P(A_t^{(i)}|Y_{0:t-1}^{(i)})$ 
18   forall the  $j \in (1, \dots, M-1) \setminus i$  do
19      $P(A_t^{(j)}|Y_{0:t}) = P(A_t^{(i)}|Y_{0:t})$ 
20      $P(A_t^{(j)}) = P(A_t^{(i)})$ 
21      $P(O^{(j)}|Y_{0:t}^{(i)}) \leftarrow \sum_{A^{(j)}} P(A_t^{(j)}, O^{(j)}|Y_{0:t}^{(i)})$  ;    ▷ object  $j$  marginal
22 else
23   forall the  $i \in (1, \dots, M)$  do
24     measurement update Algo. 2

```

The exchange of information of one joint distribution to another is achieved through the agent's marginals $A^{(i)}$ according to Algorithm 3. The measurement update is the same as previously described in Algorithm 2 in the case of no positive measurements of the objects. If the agent senses an object, all of the agent marginals of the remaining joint distributions are set to the marginal of the joint distribution pair belonging to the positive measurement $Y_t^{(i)}$.

Figure 5.14, depicts the process of information exchange between object $O^{(1)}$ and $O^{(2)}$ in the event that the agent gets a positive sensation of $O^{(2)}$. Prior to the positive detection both marginals $P(A_t^{(1)}|Y_{0:t-1}^{(1)})$ and $P(A_t^{(2)}|Y_{0:t-1}^{(2)})$ occupy the same region and are identical. When the agent senses $O^{(2)}$ the line defined by the measurement likelihood function $P(Y_t^{(2)}|A_t^{(2)}, O^{(2)})$ becomes a hard constraint implying that both the agent and $O^{(2)}$ have to satisfy this constraint.

Figure 5.15 shows marginals resulting from the joint distributions in Figure 5.14. The marginals in the *left* plot are the result after updating the marginals

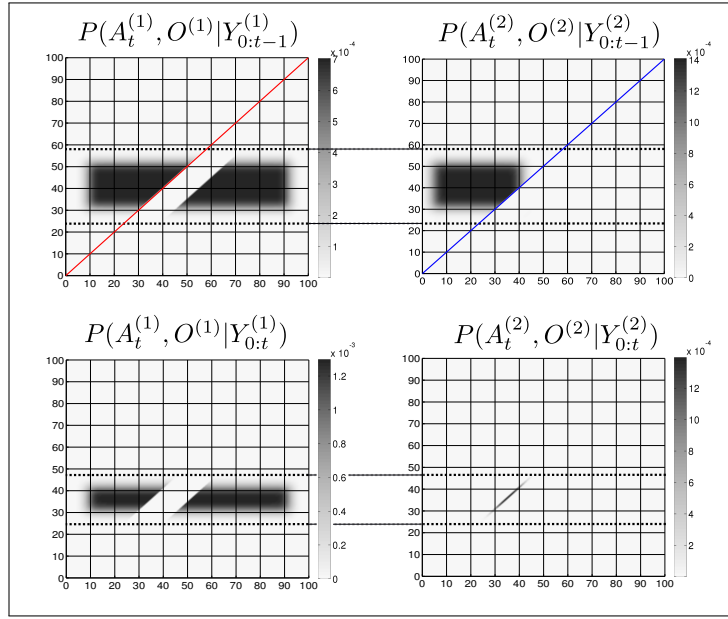


Figure 5.14: Transfer of information between joint distributions *top left and right:* Joint distributions of $P(A_t^{(1)}, O^{(1)} | Y_{0:t-1}^{(1)})$ and $P(A_t^{(2)}, O^{(2)} | Y_{0:t-1}^{(2)})$ prior and post sensing. The red and blue lines correspond to the region in which the measurement functions $P(Y_t^{(1)} | A_t^{(1)}, O^{(1)})$ and $P(Y_t^{(2)} | A_t^{(2)}, O^{(2)})$ will change the joint distributions prior and post sensing. *bottom right:* After the agent has sensed $O^{(2)}$, all the probability mass which was not overlapping the blue line becomes an infeasible solution to the agent and object locations. *bottom left:* The constraint imposed by the measurement likelihood function of the second object (blue line) is transferred to the joint distribution of the first object according to Algorithm 3. The result is a change in the joint distribution $P(A_t^{(1)}, O^{(1)} | Y_{0:t}^{(1)})$, which satisfies the constraints imposed by the agent's marginal from the joint distribution $P(A_t^{(2)}, O^{(2)} | Y_{0:t}^{(2)})$.

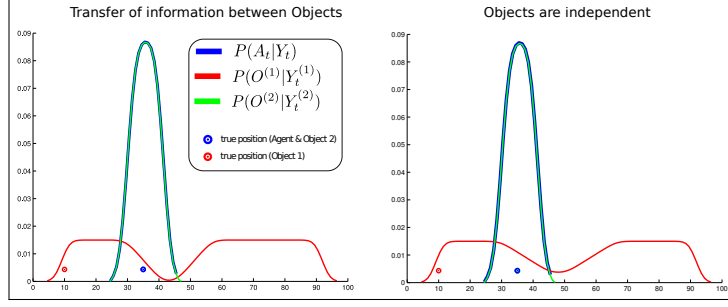


Figure 5.15: Independence & Objects *left*: resulting marginals after setting the agent marginals of each joint distribution equal $A_t^{(1)} = A_t^{(2)}$ according to Algorithm 3. The object marginal $P(O^{(2)}|Y_{0:t})$ is recomputed. *right*: resulting marginals in which the objects have no influence on one another. Note that a transfer of information has caused a change in the marginal $O^{(1)}$.

	space	time
Histogram	$\mathcal{O}(N^M)$	$\mathcal{O}(N^M)$
MLMF	$\mathcal{O}(M N)$	$\mathcal{O}(N^{(M-1)})$
scalable-MLMF	$\mathcal{O}(M N)$	$\mathcal{O}(M N)$

Table 5.2: Time and space complexity summary For both MLMF and scalable-MLMF the worst case scenario is reported for the space complexity.

$A^{(i)}$. The *right* plot shows the result for the case where the objects remain independent.

The result of introducing a dependency between the objects through the agent’s marginals in the event of a sensing and treating them independently gives the same solution as the histogram filter in this particular case. However as each individual marginal $A_t^{(i)}$ diverges from the other marginals the filtered solution will diverge from the histogram’s solution. We assume however that the objects are weakly dependent and sharing information during positive sensing events is sufficient. In section 5.5.2 we will evaluate the independence assumption with respect to the histogram filter.

Table 5.2 summarises the time and space complexity for the three filters.

5.5 Evaluation

We conduct three different types of evaluation to quantify the scalability and correctness of the scalable-MLMF filter. The first experiment tests the scalability of our filter in terms of processing time taken per motion-measurement update cycle. The second experiment evaluates the independence assumption between the objects which was made in the scalable-MLMF filter. The third and final experiment determines the effect the memory size has on a search policy to locate all the objects in the *Table* world.

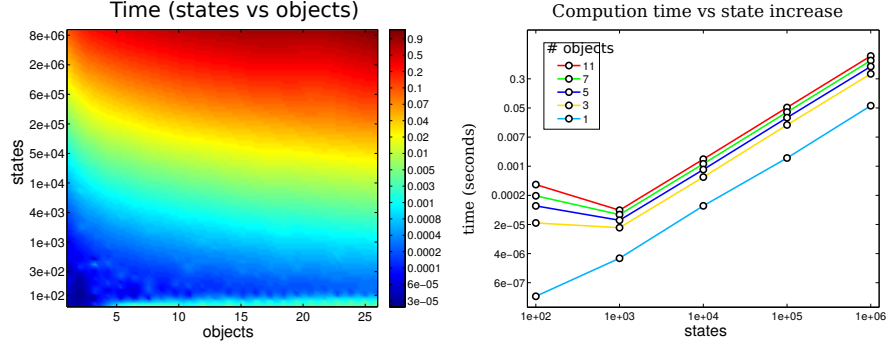


Figure 5.16: Time complexity: *left:* mean time taken for a loop update (motion and measurement) as a function of the number of states in a marginal and the number of objects present. *right:* time taken for a loop update with respect to the number of states in the marginal. The colour coded lines are associated with the number of objects present. The computational cost is plotted on a log scale. As the number of states increases exponentially the computational cost matches it.

5.5.1 EVALUATION OF TIME COMPLEXITY

We measured the time taken by the motion-measurement update loop, as a function of the number beliefs and number of states per belief. We started with a 100 states per belief and gradually increase it to 10'000'000 over 50 steps. Each of the 50 steps treated 2 to 25 objects. Figure 5.16 *left* illustrates the computational cost as a function of number of states and objects. For each state-object pair 100 motion-measurement updates were performed. Most of the trials returned time updates below 1 Hz. Figure 5.16 *right* shows the computational cost as a function of the number of states plotted for 6 different filter runs with a different number of objects. As the number of states increases exponentially so does the computational cost. Note the cost increases at the same rate as the number of states meaning that the computational complexity is linear with respect to the number of states. This result is in agreement with the asymptotic time complexity.

5.5.2 EVALUATION OF THE INDEPENDENCE ASSUMPTION


In section 5.4.5 we made the assumption (for scalability reasons) that the objects' beliefs are independent of one another. This assumption is validated by comparing the MLMF filter on three random variables, an agent and two objects, with the ground truth which we obtain from the standard histogram filter. For each of the three beliefs (the agent and two objects), 100 different marginals were generated and the true locations (actual position of the agent and objects) were sampled. The agent carried out a sweep of the state space for each of the marginals and the policy was saved and run with the scaled-

MLMF filter. In the first experiment we assumed that the objects are completely independent and that there was no transfer of information between the pair-wise joint distributions. In the second and third experiments there is an exchange of information as described in Algorithm 3. Here we compare the effect of using the product of the agent’s marginals $P(A_t|Y_{0:t}) = P(A_t^{(1)}|Y_{0:t}^{(1)}) \cdot P(A_t^{(2)}|Y_{0:t}^{(2)})$ with their average $P(A_t|Y_{0:t}) = \frac{1}{2}P(A_t^{(1)}|Y_{0:t}^{(1)}) + \frac{1}{2}P(A_t^{(2)}|Y_{0:t}^{(2)})$.

For each of the 100 sweeps the ground truth is compared with the scalable-MLMF using the Hellinger distance (Equation 5.5.1)

$$H(P, Q) = \frac{1}{\sqrt{2}} \|\sqrt{P} - \sqrt{Q}\|_2 \quad (5.5.1)$$

which is a metric which measuring the distance between two probability distributions. Its value lies strictly between 0 (the two distributions are identical) and 1 (no overlap between them). Figure 5.17 shows the kernel density distribution of the Hellinger distances taken at each time step for all 100 sweeps.

The best results were for  3). The *bottom plots* show that the Hellinger distance distribution between the object marginals for both case 2) and 3) are the same. However there is a significant improvement when using the average of the agent’s marginals as opposed to their product.

5.5.3 EVALUATION OF MEMORY

The memory is the list of all measurement likelihood functions which have been applied on the joint distribution since initialisation. As detailed previously there can be no more than N different measurement likelihood functions added to memory. In the case of a very large state space this might be cumbersome. We investigate how restricting the memory size can impact on the decision process in an Active-SLAM setting. Given our set up we choose a breadth-first search in the action space with a one time step horizon, making it a greedy algorithm. The objective function we utilise is the information gain of the beliefs after applying an action (Equation 5.5.2).

$$u_t = \arg \max_{u_t} H\{P(A_{t-1}, O|Y_{0:t-1}, u_{1:t-1})\} - \mathbb{E}_{Y_t} [H\{P(A_t, O|Y_{0:t}, u_{1:t})\}] \quad (5.5.2)$$

For each action we run the filter forward in time and consider all future measurements since we cannot know ahead of time the actual measurement. The information gain is the difference between the current entropy (defined by $H\{\cdot\}$) and the future entropy after the simulated motion and measurement update. The action with the highest information gain is subsequently selected. This is repeated at each time step. Figure 5.18 illustrates the environment setup for a 1D and 2D case. The agent’s task is to find the objects in the environment.

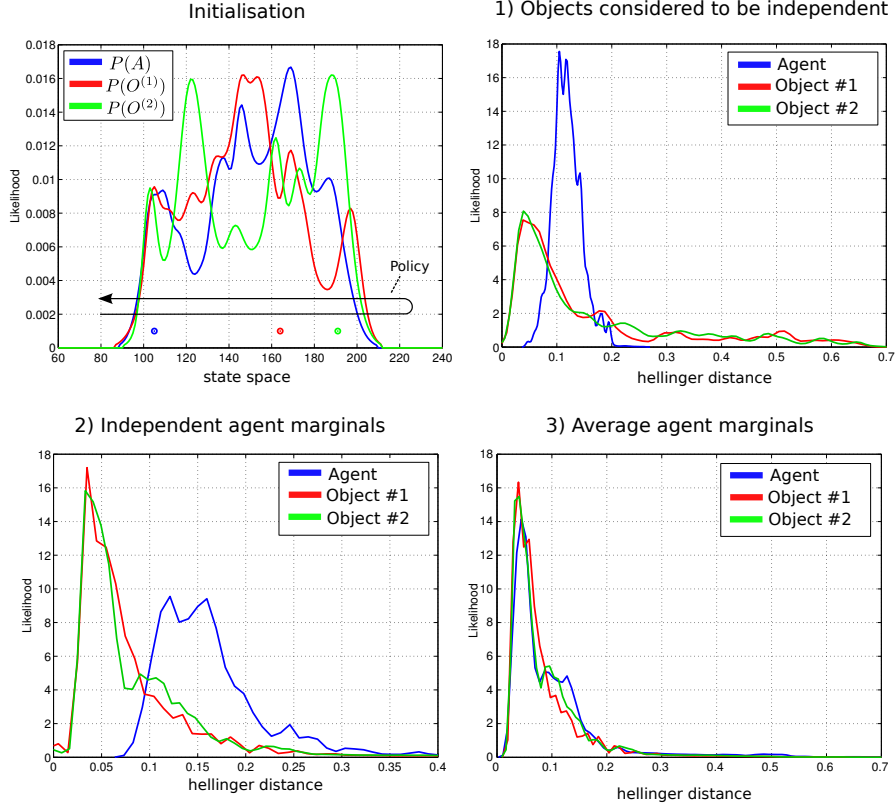


Figure 5.17: Comparison of scalable-MLMF and the histogram filter A deterministic sweep policy was carried out for 100 different initialisations of the agent and object beliefs. *top left*: One particular Initialisation of the agent and object random variables. The true position of the agent and objects were sampled at random. The black arrow indicates the general policy which was followed for each of the 100 sweeps. These were performed for 1) scalable-MLMF with objects considered to be independent at all times (no Algorithm 3). 2) Agent marginal $P(A_t|Y_{0:t})$ is the product of marginals $P(A_t^{(i)}|Y_{0:t}^{(i)})$ (Equation 5.4.15). 3) marginal $P(A_t|Y_t)$ is taken to be the average of all marginals $P(A_t^{(i)}|Y_{0:t}^{(i)})$ (Equation 5.4.16). For each of these three experiment we report the kernel density estimation over the Hellinger distances taken at every time step between ground truth (from histogram filter) and scalable-MLMF.

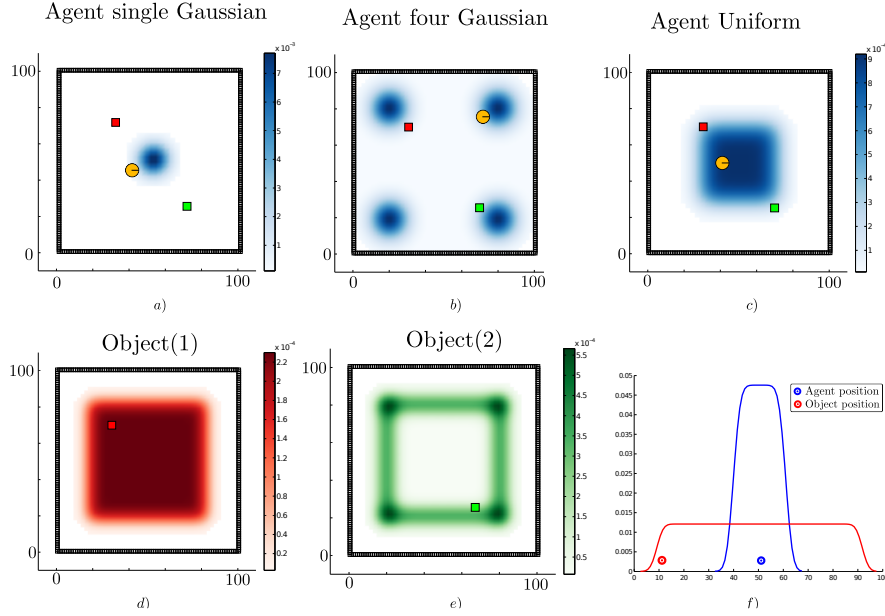


Figure 5.18: Agent's prior beliefs. Two types of environment, the first is a 2D world where the agent lives in a square surrounded by a wall whilst the second is a 1D world. In the 2D figures the agent is illustrated by a circle with a bar to indicate its heading. The true location of the objects are represented by colour coded squares. *Top row* three different initialisations of the agent's location. *Bottom row* d) the agent's prior beliefs with respect to the location of the first object and e) belief of the second object's location. *bottom row* f) 1D world with one object.

For the 2D search we consider three different initialisations (single-Gaussian, four-Gaussian, Uniform) for the agent's belief where there are two objects to be found. Ten searches were carried out for each of the three initialisations of the agent's beliefs. The agent's true location, for each search, is sampled from its initial belief, and the objects' locations (red and green squares in Figure 5.18) are kept fixed throughout all searches. We repeated each search for 18 different memory sizes ranging from 1 to N (the number of states). For the 1D search case we considered one object since adding more objects would make the search easier. We are interested in how the memory effects the search and not the search itself. In Figures 5.19-5.20 we report on the time taken to find all objects with respect to a given memory size which is shown as the percentage of the total number of states. In the 1D search case the variability of time taken to find the object converges when the memory size is at 60% of the original state space. As for the 2D search with 2 beliefs (agent & 1 object) the convergence depends on the agent's initial belief. For the 1-Gaussian (green line) all searches take approximately the same amount of time after a memory size of 9%. As for the remaining two initialisations convergence is achieved at 48%. The same holds true for the case of 3 beliefs (agent & 2 objects).

In the 2D searches, the memory size has a less impact on the time taken to find the objects than in the 1D (which is a special search case). Only when the

1D & 2 Beliefs

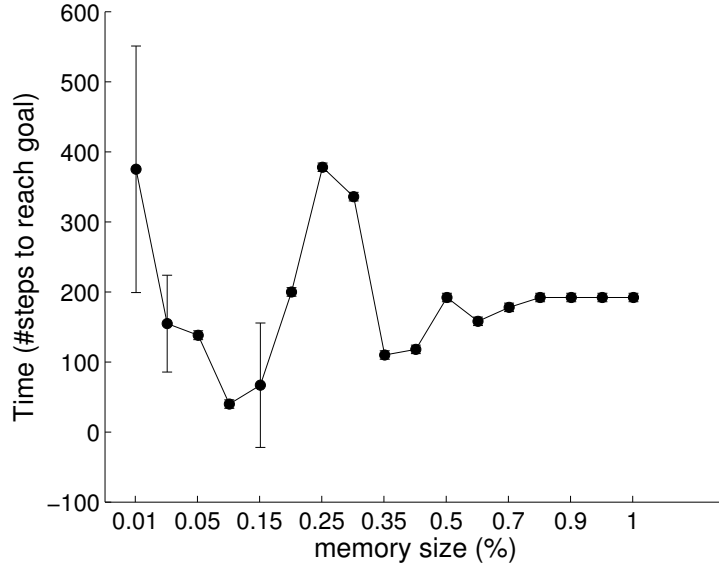


Figure 5.19: Memory size vs time to find object in 1D Results of the effect of the memory size on the decision process. The memory size is reported as the percentage of total number of states present in the marginal space. At 100% the size of the memory is equal to that of the state space. results of the 1D search illustrated in Figure 5.18 *f*).

memory size is less than 6% is there a significant change. We conclude that at least in the case of the greedy one step-look ahead planner which is frequently used in the literature, the size of the memory seems not to be a limiting factor in terms of the time taken to accomplish the search.

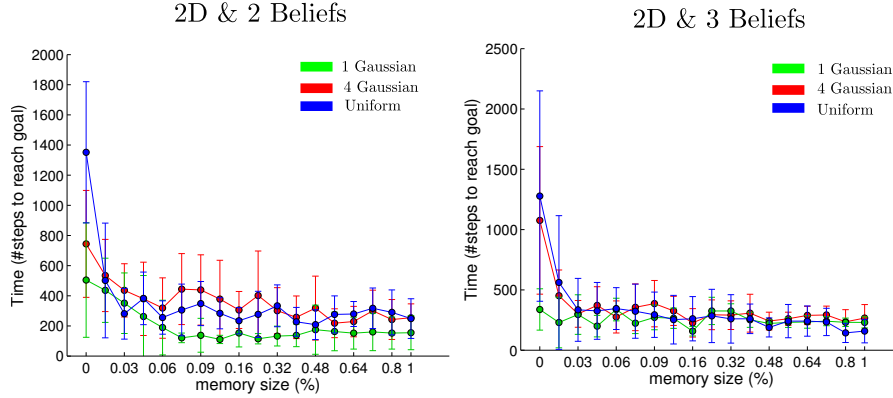


Figure 5.20: Memory size vs time to find objects in 2D. 2D search with initialisations accordingly depicted in Figure 5.18.

5.6 Conclusion

This work addresses the Active-SLAM filtering problem for scenarios in which sensory information relating to the map is very limited. Current SLAM algorithms filter the errors originating from sensory measurements and not prior uncertainty. By making the assumption that the joint distribution of all the random variables is a multivariate Gaussian, inference is tractable. Since the origin of our uncertainty does not originate from the measurement noise, we cannot assume the joint distribution to have any special structure. A suitable filter in this case would be the histogram which makes no assumption about the shape or form taken by the joint distribution. However, the space and time complexity are exponential with respect to the number random variables and this is a major limiting factor for scalability.

The main contribution of this work is a formulation of a histogram Bayesian state space estimator in which the computational complexity is both linear in time and space. We have taken a different approach to other SLAM formulations in the sense that we did not explicitly parameterise the joint distribution but kept all parameterisation in the space of the marginals (beliefs), avoiding the exponential increase in parameter space which would otherwise have been the case. Our filter’s parameters consist of the marginals and the history of measurement functions which have been applied. By solely evaluating the joint distribution at the states which are affected by the current measurement function whilst taking into account the memory, the MLMF filter obtains the same filtered marginals as the histogram filter. Further, the worst case space complexity is linear rather than exponential and the time complexity remains exponential but increases at lower rate than in the histogram filter. In striving to make the filter scalable we assume an independence assumption between the objects. An individual MLMF filter was used for each agent-object pair. We evaluated the difference between the scalable-MLMF filter with a ground truth provided by the histogram filter

for 100 different searches with respect to the Hellinger distance. We conclude that the divergence was relatively small and thus the scalable-MLMF filter provides a good approximation to the true filtered marginals. We evaluated the time taken to perform a motion-update loop for different discretisations of the state space (100 to 10'000'000 states) and number of objects (2 to 25). In most of the cases we achieved an update cycle rate below 1Hz. We evaluated how the increase of the number of states effected the computational cost. The relationship was found to be linear and thus in agreement with our analysis of the asymptotic growth rate. We analysed the effect of the memory size (the remembered number of measurement likelihood functions) on the decision theoretic process of reducing the uncertainty of the map and agent during a search task. We found that in the 2D case the memory size has much less effect than in the 1D case and we conclude that it is unnecessary to remember every single measurement function.

The implications of the MLMF and scalable-MLMF filter are that we have a computationally tractable means of performing SLAM in a case scenario in which mostly negative information is present and the joint distribution cannot be assumed to have any specific structure. The filter can be used at a higher cognitive level than processing raw sensory information as it is often in Active-SLAM. It would be well suited for reasoning tasks where the robot's field of view is limited.

An interesting future extension would be to make the original MLMF filter scalable without introducing assumptions. One possibility could be to consider Monte Carlo integration methods for inference. These can scale well to high dimensional spaces whilst still providing reliable estimates. A second possibility could be to investigate the use of Gaussian Mixtures as a form of parameterisation of the marginals so that it might be possible to blend our filter with EKF-SLAM. This would allow the parameters to grow quadratically with respect to the dimension of the marginal space as opposed to exponentially as it is in the case with the histogram and MLMF filters.

5.7 Appendix

5.7.1 BAYESIAN FILTERING RECURSION

Joint distribution

$$P(A_{0:t}, O, Y_{0:t} | u_{1:t}) = P(A_0)P(O)P(Y_0|A_0, O) \prod_{t=1}^t P(A_t|A_{t-1}, u_t)P(Y_t|A_t, O) \quad (5.7.1)$$

$$P(A_t, O, Y_{0:t} | u_{1:t}) = \sum_{A_{0:t-1}} P(A_t, A_{0:t-1}, O, Y_{0:t} | u_{1:t}) \quad (5.7.2)$$

Filtering problem

We derive $P(A_t, O | Y_{0:t}, u_{1:t})$, we start from the joint distribution, Equation 5.7.3:

$$P(A_t, O, Y_{0:t} | u_{1:t}) = \sum_{A_{t-1}} P(A_t, A_{t-1}, O, Y_t, Y_{0:t-1} | u_t, u_{1:t-1}) \quad (5.7.3)$$

$$P(A_t, O, Y_{0:t} | u_{1:t}) = \sum_{A_{t-1}} \frac{P(Y_t | \cancel{Y_{0:t-1}}, A_t, \cancel{A_{t-1}}, O, \cancel{u_t}, \cancel{u_{1:t-1}})}{P(A_t | A_{t-1}, \cancel{O}, u_t, \cancel{Y_{0:t-1}}, \cancel{u_{1:t-1}})} P(A_{t-1}, O, Y_{0:t-1} | \cancel{u_t}, u_{1:t-1})$$

$$P(A_t, O, Y_{0:t} | u_{1:t}) \quad (5.7.4)$$

$$= \sum_{A_{t-1}} P(Y_t | A_t, O) P(A_t | A_{t-1}, u_t) P(A_{t-1}, O, Y_{0:t-1} | u_{1:t-1})$$

$$= P(Y_t | A_t, O) \underbrace{\sum_{A_{t-1}} P(A_t | A_{t-1}, u_t) P(A_{t-1}, O, Y_{0:t-1} | u_{1:t-1})}_{P(A_t, O, Y_{0:t-1} | u_{1:t})} \quad (5.7.5)$$

$$P(A_t, O, Y_{0:t} | u_{1:t}) = P(Y_t | A_t, O) P(A_t, O, Y_{0:t-1} | u_{1:t})$$

$$= P(Y_t | A_t, O) P(A_t, O | Y_{0:t-1}, u_{1:t}) P(Y_{0:t-1} | u_{1:t}) \quad (5.7.6)$$

All the cancellations come from the *Markov Assumption* read from the structure of the Bayesian network. The resulting final Bayesian recursion is obtained by conditioning on the measurement and actions, which is the normalisation factor.

$$P(A_t, O | Y_{0:t}, u_{1:t}) = \frac{P(Y_t | A_t, O) P(A_t, O | Y_{0:t-1}, u_{1:t}) P(Y_{0:t-1} | u_{1:t})}{P(Y_{0:t} | u_{1:t})}$$

$$= \frac{P(Y_t | A_t, O) P(A_t, O | Y_{0:t-1}, u_{1:t}) \cancel{P(Y_{0:t-1} | u_{1:t})}}{P(Y_t | Y_{0:t-1}, u_{1:t}) \cancel{P(Y_{0:t-1} | u_{1:t})}} \quad (5.7.7)$$

$$P(A_t, O | Y_{0:t}, u_{1:t}) = \frac{P(Y_t | A_t, O) P(A_t, O | Y_{0:t-1}, u_{1:t})}{P(Y_t | Y_{0:t-1}, u_{1:t})} \quad (5.7.8)$$

$$P(Y_t|Y_{0:t-1}, u_{1:t}) = \sum_{A_t} \sum_O P(Y_t|A_t, O)P(A_t, O|Y_{0:t-1}, u_{1:t}) \quad (5.7.9)$$

$$= \sum_{A_t} \sum_O P(Y_t, A_t, O|Y_{0:t-1}, u_{1:t}) \quad (5.7.10)$$

5.7.2 RECURSION EXAMPLE

Derivation of the filtered joint distribution, $P(A_t, O, Y_t|Y_{0:t}, u_{1:t})$, for two updates. At initialisation when no action has yet been taken the filtered distribution is:

$$P(A_0, O, Y_0) = P(O)P(A_0)P(Y_0|A_0, O) \quad (5.7.11)$$

The a first action, u_1 is applied, which to get the filtered joint distribution is marginalised:

$$P(A_1, O, Y_0|u_1) = P(O) \sum_{A_0} P(A_1|A_0, u_1)P(A_0)P(Y_0|A_0, O) \quad (5.7.12)$$

$$= P(O) \sum_{A_0} P(A_1, A_0, Y_0|u_1, O) \quad (5.7.13)$$

$$= P(O)P(A_1, Y_0|u_1, O) \quad (5.7.14)$$

$$= P(O)P(A_1|u_1)P(Y_0|A_1, O) \quad (5.7.15)$$

After the application of the first action, the filtered joint has the following form:

$$P(A_1, O, Y_0|u_1) = P(O)P(A_1|u_1)P(Y_0|A_1, O) \quad (5.7.16)$$

A second measurement Y_1 and action u_2 are integrated into the filtered joint distribution:

$$P(A_2, O, Y_{0:1}|u_{1:2}) = P(O) \sum_{A_1} P(A_2|A_1, u_2)P(A_1)P(Y_0|A_1, O, u_1)P(Y_1|A_1, O) = \quad (5.7.17)$$

$$P(O) \sum_{A_1} P(A_2, A_1|u_2)P(Y_0|A_1, O, u_1)P(Y_1|A_1, O) \quad (5.7.18)$$

$$P(O)P(A_2|u_{1:2})P(Y_0|A_2, O)P(Y_1|A_2, O) \quad (5.7.19)$$

Repeating the above for $Y_{2:t}$ and $u_{3:t}$ results in:

$$P(A_t, O, Y_{0:t}|u_{1:t}) = P(O)P(A_t|u_{1:t}) \prod_{i=0}^t P(Y_i|A_t, O) \quad (5.7.20)$$

5.7.3 DERIVATION OF THE EVIDENCE

The evidence, also known as the marginal likelihood, is the marginalisation of all non measurement random variables from the filtered joint distribution $P(A_t, O, Y_{0:t} | u_{1:t})$. We detail below how we compute the evidence in a recursive manner whilst only considering dependent regions of the joint distribution.

We start with the definition of the evidence (we dropped $u_{1:t}$ to simplify the notation).

$$P(Y_{0:t}) = \sum_{A_t} \sum_O P(A_t, O, Y_{0:t}) \quad (5.7.21)$$

As we are interested in a recursive computation of the evidence, we consider the gradient:

$$\alpha_t = \nabla_{Y_t} P(Y_{0:t}) = P(Y_{0:t}) - P(Y_{0:t-1}) \quad (5.7.22)$$

$$\alpha_t = \sum_{A_t} \sum_O P(A_t, O, Y_{0:t}) - P(A_t, O, Y_{0:t-1}) \quad (5.7.23)$$

$$= \sum_{A_t} \sum_O P(Y_t | A_t, O) P(A_t, O, Y_{0:t-1}) - P(A_t, O, Y_{0:t-1}) \quad (5.7.24)$$

$$= \sum_{A_t} \sum_O (P(Y_t | A_t, O) - 1) P(A_t, O, Y_{0:t-1}) \quad (5.7.25)$$

The gradient α_t is the difference in mass before and after the application the likelihood function, $P(Y_t | A_t, O)$. The above summation, Equation 5.7.25, is over the entire joint distribution state space. We can take advantage of the fact that the likelihood function is sparse and will only affect a small region of the joint distribution, which we called the dependent states, \cap . The states which are not affected by the joint distribution will result in a contribution of zero to Equation 5.7.25. We rewrite the gradient update in terms of only the dependent regions:

$$\alpha_t = \sum_{A_t} \sum_O (P(Y_t | A_t, O) - 1) P_{\cap}(A_t, O, Y_{0:t-1}) \quad (5.7.26)$$

Consider the first update of the evidence at time $t = 0$:

$$\alpha_0 = \sum_{A_0} \sum_O (P(Y_0 | A_0, O) - 1) P(A_0, O) \quad (5.7.27)$$

The one in Equation 5.7.28 is the original value of the normalisation denominator before any observation is made and as the initial joint distribution $P(A_0, O)$ is normalised the value of the denominator is one.

$$P(Y_0) = 1 + \alpha_0 \quad (5.7.28)$$

For the evidence $P(Y_{0:t})$ we consider the summation of all the derivatives α_t

from time $t = 0$ until t :

$$P(Y_{0:t}) = 1 + \sum_{t=0}^t \alpha_t \quad (5.7.29)$$

5.7.4 DERIVATION OF THE MARGINAL

The marginal of a random variable is the marginalisation or integration over all other random variables, $P(A_t, |Y_{0:t}) = \sum_O P(A_t, O | Y_{0:t})$. Below we give a form of this integration which exploits the independent regions in the joint distribution.

$$P(A_t, |Y_{0:t}) = \mathbf{P}(\mathbf{A}_t | \mathbf{Y}_{0:t-1}) - \left(\mathbf{P}(\mathbf{A}_t | \mathbf{Y}_{0:t-1}) - P(A_t | Y_{0:t}) \right) \quad (5.7.30)$$

In Equation 5.7.30 we add and subtract $P(A_t | Y_{0:t-1})$ and we further split $P(A_t | Y_{0:t-1})$ into independent and dependent components:

$$P(A_t, |Y_{0:t}) = P(A_t | Y_{0:t-1}) - \left(\underbrace{P_{\cap}(A_t | Y_{0:t-1}) + \cancel{P_{\ominus}(A_t | Y_{0:t-1})}}_{P(A_t | Y_{0:t-1})} - \underbrace{P_{\cap}(A_t | Y_{0:t}) + \cancel{P_{\ominus}(A_t | Y_{0:t})}}_{P(A_t | Y_{0:t})} \right) \quad (5.7.31)$$

From equation 5.7.31 to 5.7.32 we used the fact that independent regions of the marginal distributions will remain unchanged after an observation, $P_{\ominus}(A_t | Y_{0:t-1}) = P_{\ominus}(A_t | Y_{0:t})$, and before re-normalisation. This results in the final recursive update:

$$P(A_t, |Y_{0:t}) = P(A_t | Y_{0:t-1}) - \left(P_{\cap}(A_t | Y_{0:t-1}) - P_{\cap}(A_t | Y_{0:t}) \right) \quad (5.7.32)$$

Equation 5.7.32 states that only elements of the marginals which are dependent will change by the difference of before and after a measurement update.